Woody species diversity using remote sensing and environmental data with Neural Network

Mohammad Redowan
March, 2010

Course Title:	Geo-Information Science and Earth Observation for Environmental Modelling and Management
Level:	Master of Science (MSc)
Course Duration:	September 2008 - March 2010
Consortium partners:	University of Southampton (UK) Lund University (Sweden) University of Warsaw (Poland) International Institute for Geo-Information Science and Earth Observation (ITC) (The Netherlands)
GEM thesis number:	2010-22

Woody species diversity using remote sensing and environmental data with Neural Network

by

Mohammad Redowan

Thesis submitted to the faculty of Geo-information Science and Earth Observation, University of Twente in partial fulfilment of the requirements for the degree of Master of Science in Geo-information Science and Earth Observation for Environmental Modelling and Management

Thesis Assessment Board

Internal Examiner (Chair): Professor Andrew K. Skidmore
External Examiner: Professor Katarzyna Dabrowska
Primary supervisor: Dr. Tiejun Wang
Secondary supervisor: Dr. Hein van Gils

UNIVERSITY OF TWENTE.

ITC FACULTY OF GEO-INFORMATION SCIENCE AND EARTH OBSERVATION

Disclaimer

This document describes work undertaken as part of a programme of study at the International Institute for Geo-information Science and Earth Observation. All views and opinions expressed therein remain the sole responsibility of the author, and do not necessarily represent those of the institute.

Abstract

Most of the remote sensing studies of plant diversity focused only on one aspect of plant diversity i.e. species richness, paying limited attention to other aspect i.e. species evenness. Moreover, environmental data is comparatively less used in the studies of remote sensing plant diversity and evenness, despite having potential to increase map accuracy. This study compares the mapping accuracy of woody species diversity and evenness of an Italian forest site by using two medium resolution imageries of Landsat 5 Thematic Mapper (TM) and Advanced Land Observing Satellite (ALOS) with Neural Network classifier. The study jointly used satellite data with four other environmental variables namely elevation, slope, aspect and solar radiation in different combinations. The highest overall map accuracies obtained using TM and ALOS imageries are 60% and 53% respectively for woody species diversity and 59% and 46% respectively for woody species evenness. Use of environmental data increases the classification accuracy significantly. The highest overall map accuracies obtained by using TM and ALOS data jointly with environmental data were 91% and 81% respectively for woody species diversity and 83% and 80% respectively for woody species evenness. Landsat TM maps both woody species diversity and evenness more accurately than ALOS, with or without environmental data. Coarser pixel size and higher spectral resolution of TM proved to be contributing factors in getting higher map accuracy compared to ALOS.

Key words: Woody species diversity, woody species evenness, Shannon Diversity Index, Shannon Evenness Index, Neural Network, TM, ALOS, multicollinearity, forest types.

Acknowledgements

All praise and glory to be Him, Almighty Allah, Master of the worlds. Thanks my Lord for giving me strength and wisdom to complete this thesis.

My appreciation and gratefulness to all financial promoters of European Union (EU) for supporting the GEM program through the Erasmus Mundus (EM) scholarship scheme.

Special thanks to the consortium directors namely Professor Andrew K. Skidmore (ITC), Professor Terry Dawson (University of Southampton), Professor Peter Pilesjõ (Lund University), and Professor Katarzyna Dabrowska (University of Warsaw) for institutional support and organization of the course over four institutions of four European countries. Thanks to all academic staffs of the partner institutions.

Services of program sectaries of the institutions; Stephanie Webb, Karin Larsson, Gosia and Monique Romarck were invaluable and I would say to them thank you. Course coordinator Mr. Andre Kooiman deserves special thanks for all out help through the whole duration of the course.

My heartfelt gratitude to my first supervisor Dr. Tiejun Wang and second supervisor Dr. Hein van Gils for all out effort, time and energy they spent on me to promote my thesis. I have no hesitation to tell that I feel proud and privileged getting the opportunity to work with such wonderful personalities. Dr. Wang gave me innovative ideas, taught software operations and constantly supervised the work. Dr. Hein was the kingpin in organizing and monitoring the field campaign and constantly supervised the work.

Thanks to my fieldwork colleagues Dr. Anton Vrieling, Abraham Tesfai, Desalegn Chala, Li Dai, Chia-chi Chang, Diriba Kumssa, Sylvia Nanyomo and Upenyu Naume Nyatondo for their cooperation and nice company. We are grateful to all of the staffs of Majella national park in Italy who provided us necessary support.

My GEM classmates of 2008-2010 academic session are wonderful peoples from around the world. Special thanks to all of them for supporting, good wishing, and helping me in different stages of the course and thesis.

Lastly, my gratitude to my family members, relatives and friends who have always been my inspiration.

Table of contents **Page**

List of figures **Page**

List of tables **Page**

Chapter 1: Introduction

1.1 Background

Interest to measure and model plant diversity from space is in increase (Turner et al., 2003). Biogeographers have long-cherished fervour in spatial and temporal distribution of plant diversity (Whittaker et al., 2005; Lomolino et al., 2004) particularly measuring patterns of species occurrence (Gillespie et. al., 2008). Presently remote sensing data is a potential source of information on plant diversity at landscape, regional, continental, and global spatial scales (Nagendra, 2001; Willis and Whittaker, 2002). Rapid assessment of plant diversity is crucial for management and conservation purpose (Foody, 2003; Whittaker et al., 2005) but we lack methods for rapid, large scale assessment (Bawa et al., 2002). Remote sensing provides inexpensive, extensive and complete spatial coverage for large areas that can be updated regularly (Duro et al., 2007). Despite such potential, remote sensing data has not been used much in the studies of plant diversity (Trisurat et al., 2000).

Studies on remote sensing plant diversity till today use mainly two broad approaches; direct and indirect (Turner et al., 2003; Nagendra, 2001 and as reviewed by Gillespie et al., 2008 and Duro et al., 2007). Direct approaches use remotely sensed data to identify the species e.g. individual species (Sobhan, 2007; Foody et al., 2005; Carleer and Wolff, 2004; Haara and Haarala, 2002), invasive species (Ramsey et al., 2005; Hunt et al., 2004; Parker-Williams and Hunt, 2004; Hunt et al., 2003), weed (Everitt et al. 2006; Carson et al 1995), mangrove species (Dahdouh-Guebas et al., 2004; Wang et al., 2004b), broad land cover types (Nagendra and Gadgil, 1999a; Nagendra and Gadgil, 1999b; Martin et al., 1998), or assemblage pattern of species diversity (Foody and Cutler, 2006; Nagendra and Gadgil, 1999a) and directly map their distribution. Indirect approaches model the species distribution (Saatchi et al., 2008) and distribution of diversity indices e.g. Shannon diversity index (SDI) (Bawa et al., 2002), Fisher's alpha (Saatchi et al., 2008; Cayuela et al., 2006).

Information on plant diversity from the remotely sensed data can be extracted in versatile manners. Many researchers have used vegetation index NDVI and regression analysis (e.g. Levin et al., 2007; Rocchini, 2007; Gillespie 2006; Carter et al., 2005; Fairbanks and McGwire, 2004; Waser et al., 2004; Oindo and Skidmore 2002; Gould, 2000). Few authors used spectral heterogeneity of remotely sensed data (Spectral Variation Hypothesis-SVH) to assess habitat heterogeneity/plant diversity (e.g. Rocchini, 2007; Rocchini et al., 2007; Palmer et al., 2002). Other authors used surrogate data, for example vegetation maps (e.g Lauver and Whistler 1993; Griffiths et al., 2000; Luoto et al., 2002). Wang et al., (2004) mapped different assemblage of mangrove species in the Caribbean coast of Pannama by applying an integrated approach of pixel-based and object-oriented classification. However these conventional image analysis techniques of species diversity estimation may not always be appropriate and does not fully exploit the data's information content (Foody and Cutler, 2006).

Neural Network (NN) is a promising image classification method used by many investigators. (e.g. Foody and Cutler, 2006; Augusteijn and Warrender, 1998; Skidmore et al., 1997; Mutanga and Kumar, 2007). NN performs general land-cover classification with better accuracy than other conventional methods e.g. maximum likelyhood (Hepner et al., 1989; Civco, 1993). The advantage of NN is that it is non-parametric classifier and ancillary environmental data can be fed to the classifier along with satellite data.

Many researchers have long recognized the striking variability of plant diversity with many environmental factors. Effect of elevation on vegetation is known over a century (Lomolino, 2001; Wallace, 1878). Increased topographic relief compared to flatter regions are associated with increased species diversity (O'Brien et al., 2000; Richerson and Lum, 1980). Bolstad et al., (1998) and Tivy (1993) observed strong relationship between some species and elevation and/or terrain shape. Currie and Paquin (1987) reported energy to be a major determinant of species diversity. Currie (1991) and Pierce et al., (2005) found solar radiation and potential evapotranspiration strongly related with plant diversity. Therefore environmental data e.g. slope (surface gradient), aspect (surface orientation), elevation (surface altitude), solar radiation (sunshine or direct radiant energy to which a region is exposed) etc has great potential to explain the variation in species distribution pattern and diversity (Zhang et al., 2007; Vogiatzakis et al., 2006). Unfortunately, potential of these various environmental factors are less utilized in the studies of remote sensing plant diversity.

Biological diversity is a multifaceted variable and difficult to measure and express simply (Duro et al., 2007). Complexities of biological communities are often described and generally understood in terms of two integral components; species diversity and evenness (Gillespie et al., 2008; Drobner et. al., 1998; Whittaker, 1965; Tilman, 1996; Stirling and Wilsey, 2001). Species diversity is the number of different species in a particular area (species richness) weighted by some measure of abundance such as number of individuals or biomass. But species richness is neither a synonym nor a measure of species diversity (Sanjit and Bhatt, 2005), although it has been widely used in most of the related studies as proxy to species diversity. Species evenness is the relative abundance or equitability (Izsa´k, 2007) with which each species is represented in an area. Evenness is also defined as the proportion or percentage of organisms in a community or simply the way abundance is distributed among individual species in a community (Whittaker, 1975; Alatalo, 1981). A biological community where all the species are represented by the same number of individuals has high species evenness. A biological community where some species are represented by many individuals, and other species are represented by few individuals has low species evenness. Most species in nature are moderately abundant, some are very abundant or extreme rare. Summarily, diversity technically refers to a combination of species richness weighted by a measure of abundance, which is generally quantified as an index e.g. Shannon diversity index (H), Simpson index or Fisher's alpha (Gillespie et al., 2008); and evenness indicate species relative abundance which is also quantified by an index such as Shannon evenness index (E) (see formula in section 2.3.5). Diversity indices provide more information on species variation and composition, and not only the species richness (Tolera et al., 2008).

1.2 Problem statement

Very few studies concern evenness

Till today, most of the remote sensing studies have mainly focused on only one aspect of plant diversity and that is species richness (Foody and Cutler, 2006) paying limited attention to other aspect and that is species evenness (Schmidtlein and Sassin, 2004; Foody, and Cutler, 2003). But species evenness is equally important (Purvis and Hector, 2000). No study of remote sensing plant diversity except a few (e.g Foody and Cutler, 2006) concerns both species diversity and evenness as this study does to bridge the research gap.

Image resolution, inherent capacity and spatial scale

Landscape level studies of plant diversity used medium resolution imageries from e.g. TM, ETM+, ASTER or IRS satellite/sensor by applying varying approach like image spectral heterogeneity, vegetation indices, climatic and topographic variables but with considerable level of accuracy (40 to 80%) (e.g. Nagendra, 2002; Nagendra and Gadgil, 1999; Foody and Cutler, 2006). Studies involving direct identification of species and mapping diversity used very high spatial resolution (1 to 4m) imageries from IKONOS, OrbView, OuickBird satellites or hyper-spectral airborne sensors with quite high accuracy (60 to 90%) (e.g. Sobhan, 2007; Foody et al., 2005; Carleer and Wolff, 2004). Both of the approaches incur complications. If image spatial resolution is too low, objects discrimination becomes difficult; if too high (smaller than object under consideration) intra-class variability increase and classification accuracy decrease (Meyer et al., 1996; Nagendra, 2001). Further, high spatial resolution imageries are collected primarily from commercially operating satellites which are very expensive - US$3000-5000 for 10km^2 (Gillespie et. al.,

2008) and are not affordable to developing countries. Feasible alternative to costly high resolution imageries might be the low cost, fine resolution imagery (ALOS or TM). Moreover, due to long time series of data availability (since 1982), TM offers opportunity of trend analysis in plant diversity study.

Rocchini (2007) studied the effect of image spatial and spectral resolution in estimating ecosystem α-diversity and reported that SWIR ASTER bands had shown low power in catching spectral and thus spatial variability (in turn species diversity) with respect to Landsat ETM+ imagery while both imageries posses same spatial resolution (30m). Besides, image spectral variability is scene and sensor dependent (Rocchini et al., 2007; Mehner et al., 2004). Hence we expect variation in remotely sensed spectral response and in turn species diversity would be better captured at 30m scale (TM) than at 10m scale (ALOS). Rocchini et al., (2004) noted that the number of bands used for quantifying image spectral heterogeneity may affect the accuracy of the relationship between the spectral data and species diversity. Therefore it is argued that image spatial resolution is not the only decisive factor in catching spatial heterogeneity of species diversity but also the spectral resolution. TM posses quite low spatial resolution (30m) but more bands (7) while ALOS posses a fairly high spatial resolution (10m) but fewer bands (4). Following Rocchini (2007), we anticipated that there might be a trade off between the spatial and spectral resolutions of TM and ALOS data and sensors might have differential capability in detecting variability of woody species diversity.

Therefore, present study endeavoured to compare the capability of using two differential resolutions (spatial and spectral) satellite imageries (TM and ALOS) to accurately map woody species diversity and evenness using NN classification method. Further, TM series data has been used most widely (cited in 42 articles) in the studies of plant diversity with varying approach, while ALOS data (among few others) has not been used at all (Gillespie et al, 2008). No study compared the suitability of using the most widely used (TM) image with the least used one (ALOS) for accurately mapping woody species diversity (H) and evenness (E).

Ancillary environmental data very less used

Ancillary environmental data (e.g elevation, aspect, slope, solar radiation) are useful help to better explain the variation and accuracy of remotely sensed plant diversity. Skidmore et al., (1997) reported that training accuracy of NN increases when satellite data is jointly used with ancillary environmental data. Of course, use of environmental data in the study of vegetation and landcover classification is well practice over years (e.g. Yang et al., 2007; Schmidt et al., 2004; Franklin, 1994; Franklin et al., 1994; Janssen et al., 1990; Skidmore, 1989) but not in remote sensing species diversity. Till date, very few studies have explained the effect of coupling ancillary environmental data with remotely sensed data in studies of plant diversity. To the best of our knowledge, only Cayuela, et al., (2006), modelled plant diversity using climatic, biophysical and landcover data with ETM+ NDVI using GLM. Therefore, present study investigates the effect of incorporating ancillary environmental data on mapping accuracy of woody species diversity (H) and evenness (E) by satellite data (ALOS and TM).

1.3 General Objective

The study aims to propose a new approach to estimate woody species diversity and evenness by using satellite imagery and ancillary environmental data (elevation, slope, aspect, solar radiation) with neural network classifier.

1.3.1 Specific Objectives

1) To assess the suitability of ALOS and TM imageries to accurately map woody species diversity and evenness.
2) To compare the accuracy of produced maps using TM and ALOS data.
3) To evaluate the influence of ancillary environmental data (elevation, slope, aspect, solar radiation) on the accuracy to estimate woody species diversity and evenness using satellite data.
4) To explore how woody species diversity and evenness in Majella vary with forest types and elevation.

1.4 Research questions

1. Can woody species diversity and evenness of Majella be mapped with high accuracy using TM and ALOS imageries?
2. Which image produces more accurate woody species diversity and evenness maps, TM or ALOS?
3. Does the ancillary environmental data (elevation, slope, aspect, solar radiation) significantly improve the mapping accuracy of woody species diversity and evenness by satellite data?
4. How the woody species diversity and evenness do vary with forest types and altitude gradients?

1.5 Research Hypotheses

I. TM and ALOS imageries can map woody species diversity and evenness with high accuracy.

II. Woody species diversity and evenness would be better captured at 30m spatial scale (by TM) than at 10m (by ALOS).

III. Ancillary environmental data significantly improves mapping accuracy of woody species diversity and evenness by satellite data.

IV. Woody species diversity and evenness in Majella vary with forest types and altitude.

Chapter 2: Materials and Methods

2.1 Study site

The study was undertaken over an area of 170 km^2 in the north-western part (Morrone) (42°4'30"- 42°14'40"N; 13°49'55"- 14°1'51"E) of Majella National Park, in the Abruzzo region in central Italy.

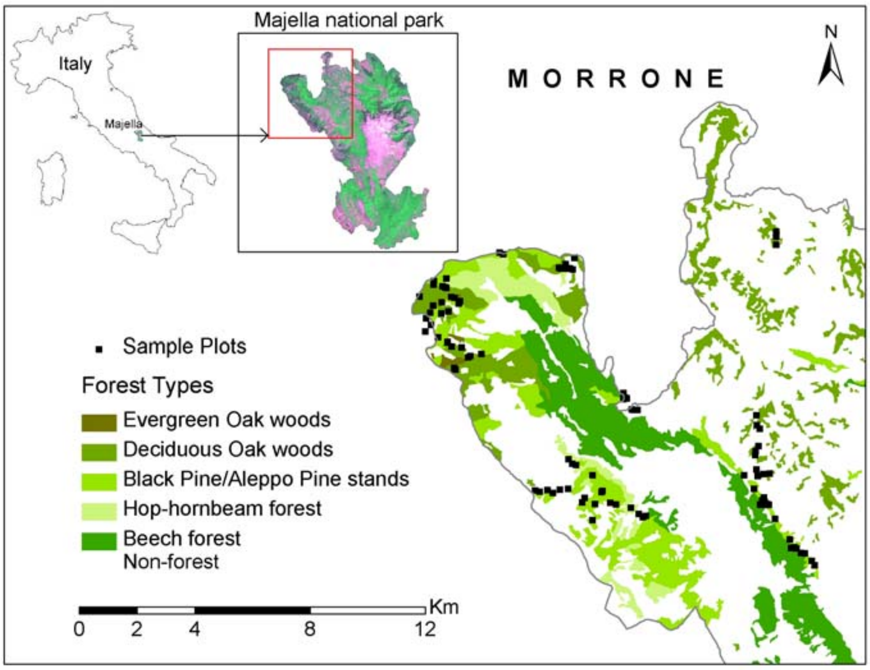

Fig 2.1: Location of study site and sample plots on various forest types, Majella national park, Italy.

Source: (Parco Nationale della Majella, 1999)

Morrone is the most forest type rich area of the park at close proximity to each other (Figure 2.1). Morrone mountain range (peak mount Morrone, 2061m a.m.s.l) passes through the western part of the park where this study site largely engulfs part of the range.

The area covers three typical phytoclimatic belts: Mediterranean (up to 500 m altitude), Submediterranean (500 to 900 m) and Montane (900 to 1600 m). Vegetation of the site is broadly classified into several prominent forest types based on the dominant species, located sparsely or contiguously in different altitudinal levels. Spatial extent of these forest types differ in magnitude; evergreen oak woods comprises 2% of the area, deciduous oak woods 31%, black/aleppo pine stands 26%, hop-hornbeam forest 13 % while beech forest extends over 28% area of the study site.

Affect of altitude on vegetation is evident in Majella. Plant diversity decreases considerably along upward altitude gradients (Stanisci et al., 2005). Below 400m, vegetation is true Mediterranean type evergreen forest with abundant Mediterranean Oak/Evergreen Oak (*Quercus* spp) patches and farmlands; at 400–1000m elevation levels, vegetation is sub-Mediterranean type (with deciduous, thermophilic forest) and mainly consists of Pubescent Oak (*Quercus pubescens*), Turkey Oak (*Quercus cerris*), different Mapple (*Acer* spp), Ash species (*Fraxinus* spp), Hop-hornbeam (*Ostrya carpinifolia*), some conifers and farmlands; at 1000 – 1700m altitude, vegetation is temperate Montane type (with deciduous, mesophilic forest) where European Beech (*Fagus sylvatica*) is the most dominant species; at altitude >1700m, subalpine vegetation with dwarf shrubs e.g. Juniper (*Juniper communis*) or shrubby Pine are found; and above 2000m elevation, vegetation is of the type Alpine with closed grassland, open herbaceous and dwarf-shrubs or bare-land and devoid of trees or shrubs. Furthermore, at altitude above 1000m, Beech (*Fagus sylvatica*) is the dominant species while below that elevation, Pubescent Oak (*Quercus pubescens*) is the dominant one (van Gils et al., 2008).

Mediterranean phytoclimatic belt of Majella possess typical Mediterranean climate with cool, moist winter and warm, dry summer (Nahal, 1981). Montane belt is characterized by low temperature, harsh winter conditions, cooler summer and high, evenly distributed rainfall than contiguous lowlands. Sub-Mediterranean belt possess warm, dry climate with frequent annual summer draught due to hot spell (July-August).

Geologically the area is largely composed of layers of limestones where all the geological eras from the Triassic are represented (Stanisci et al., 2005). Soil is Typic Rendolls (shallow calcareous soil with limestone lithology) and locally Typic and Aquic Eurochrepts (van Gils et al., 2010).

2.2 Study Materials and methods

The overall methodical approach followed in this research has been presented as a schematic diagram in Figure 2.2.

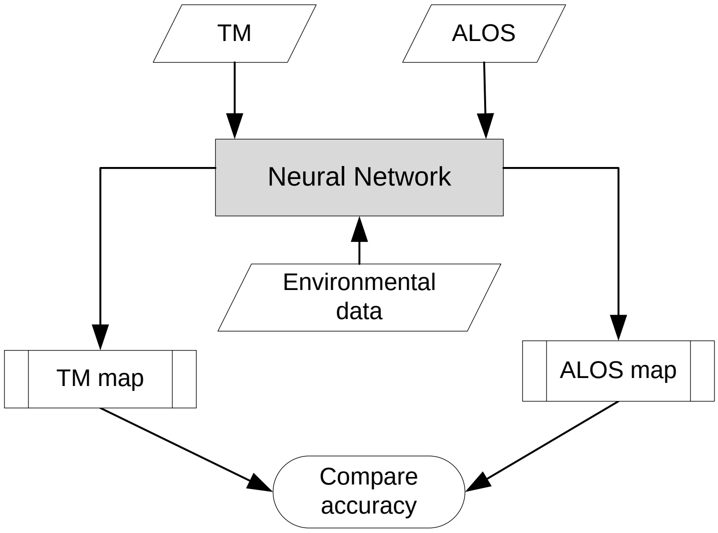

Fig 2.2: Schematic diagram of the research approach

2.2.1 Acquisition of satellite imageries and preprocessing

Two cloud and defect free satellite imageries were compared for mapping woody species diversity and evenness; ALOS Advanced Visible and Near Infrared Radiometer type 2 (AVNIR-2) (15 July 2007) and Landsat 5 Thematic Mapper (TM) imageries (27 September 2003) (Table 2.1). Both of the images have been made available for use through ITC.

Table 2.1: Characteristics of TM and ALOS used in this study.

Satellite	Spatial resolution	Spectral resolution	Acquisition date
TM	30m	6	27 Sep'03
ALOS	10m	4	15 July'07

Band no 6 of TM image was not used (some similar studies also excluded e.g. Foody and Cutler, 2006; Gould, 2000) as it is thermal waveband and not generally used in vegetation remote sensing. Therefore, Bands 1 to 5 and 7 (multispectral) of TM were used in the analysis. For the case of ALOS, all the available bands i.e. bands 1 to 4 (multispectral) were used in this study. The study site in both of the images was free from clouds and defects.

Image preprocessing includes geometric correction (geo-referencing) and atmospheric correction which had been performed by ITC remote sensing laboratory. TM and ALOS imageries were ortho-rectified to Universal Transverse Mercator (UTM) coordinates (World Geodetic System WGS 84, 33 N) using 30m resolution ASTER global DEM with the co-registration method in ERDAS 9.3.

2.2.2. Acquisition of environmental data and preprocessing

Various environmental data layers that were used in the analysis have been listed below (Table 2.2). Digital Elevation Model (DEM) data had been made available from the ASTER global DEM archive of National Aeronautic and Space Administration (NASA) through ITC. Slope angle, slope aspect and incoming solar radiation of the study site were created from the DEM using standard operations in ArcGIS 9.3 software. Solar radiation layer values of the study area were calculated for every 15 days and summed up for the whole year (Kumar et al., 1997; Currie, 1991).

Forest type map of Majella (which is a polygon layer with distinctive forest stand types) was readily obtained from the park office. Mainly five forest types relevant with the study site were extracted from many other landuse cover types of Majella included in the map which consist beech forest, deciduous oak woods, evergreen oak woods, black/aleppo pine stands and hop-hornbeam forest.

Table 2.2: Environmental data layers used in this study.

Layers	Source	Data type	Value range
Elevation*	DEM	Raster	0 to 2031 m a.s.l
Slope angle	DEM	Raster	0 to 87.33^0
Slope aspect	DEM	Raster	0 to 360 azimuth^0
Solar radiation	DEM	Raster	182981 to 1661189 Watt hr $m^{-2}year^{-1}$
Forest types thematic map**	Majella	Vector	EO, DO, BP/AP, HH, B*
Park boundary	Majella	Vector	N/A

Elevation* from ASTER global Digital Elevation Model-DEM; 30m resolution; Geocoding-ortho; vertical accuracy 7m.

Forest types** EO= Evergreen Oak; DO= Deciduous Oak; BP/AP= Black/Aleppo Pine; HH= Hop-hornbeam; B= Beech

ASTER DEM is of 30m spatial resolution, therefore, DEM and its derivatives (slope, aspect, solar radiation) needed not any resampling in case of TM data to make it correspondent to 30m×30m field plot. But for the case of ALOS, the image is of 10m spatial resolution while the DEM is of 30m spatial resolution; therefore the DEM and its derivatives (slope, aspect, solar radiation) were re-sampled to 10m spatial resolution to coincide with spatial resolution of imagery. While the four GIS environmental layers were readymade, they were layer stacked with the corresponding satellite imageries using ENVI 4.3. At this level stacked five layers are ready for feeding up to the NN for classification.

2.2.3. Instruments and accessories

The following instruments and accessories were utilized during the whole research period in the field and indoors.

a) Topographic maps: For field navigation and selection of sample plots. Copy of the map is available to buy from the Caramanico office of Majella national park.
b) GPS: iPAQ and 12 channel Garmin GPSs were used for field navigation and recording sample plot coordinates.
c) Measuring tape: For laying out sample plots and line transect in each plot.
d) Computer and software: ArcGIS 9.3, ENVI 4.3, ERDAS IMAGINE 9.3, SPSS, MS-Excel and MS- Word software was used for satellite and environmental data preparation, analysis and write up.

2.3.4 Field data collection

Field surveys were undertaken from 7th September to 30th October in 2009. Field data was collected using stratified purposive sampling with strata based on available forest types. Of course, stratified random sampling with the strata based forest types could be another alternative; but due to inaccessibility of terrain, peculiar land formations, lack of roads and walking trails through the forest at different altitude, steep slope conditions, deep gorges and after all limited logistics for mobility in the field, this option could not be undertake. Furthermore, this study intended to capture only the woody species composition in the site. Other non-woody land cover types e.g. grassland, pasture, barren land, naked hill slopes, agricultural lands and settlements that were commonly observed in the study area, were excluded from field survey. Therefore to capture the maximum variation of the woody species composition in different forest types of the study site, stratified purposive sampling strategy having sample plots in all the available forest types (evergreen oak, deciduous oak, black/aleppo pine, hop-hornbeam and beech) in proportion to their spatial extent, was the best feasible alternative in the field and applied in this study (Table 2.3).

Samples plots were collected from all available forest types involving wide range of altitude (210 to 1304 m), slope (ranging from very gentle to very steep) and aspects conditions. Although we do not have the record of the slope and aspect of all the field plots, we tried to ground sample plots at various slopes and aspects during field campaign. Furthermore, while we draped the collected sample points in a 3D image view of the study area (created using 30m resolution ASTER DEM in

ArcScene), it is seen that they are located in versatile slopes and aspects of the terrain. All together 100 sample plots were surveyed. Orientation of the plots was based on arbitrary, local topography and easiness of mobility inside the plot.

Table 2.3: Relative proportion (%) of area covered by each forest types in the study site with respective average values of Shannon diversity (H) and Evenness (E) indices for 30m plot size.

Forest types	Area covered (%)	No of sample plots
Beech	28	15
Black/Aleppo Pine	26	29
Evergreen Oak	2	7
Hop-hornbeam	13	12
Deciduous Oak	31	37

Line transect method (for details readers are referred to Runkle, 1982; Økland, 1990) was applied to each selected sample plot for recording woody species composition. Line transect method of recording species composition in the sample plots is very useful technique specially in the hilly terrains (like Majella) and recently used by many ecologists in the study of species diversity of forest ecosystems (e.g. Tolera et al., 2008; Günter et al., 2007).

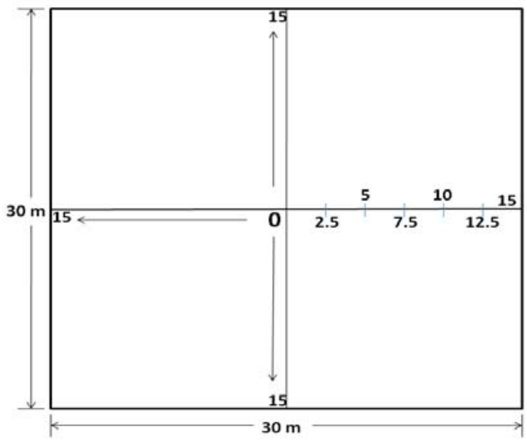

Fig 2.3: Layout specifications of line transects in each individual field sample plot

In practice, firstly, the centre point of each plot (as a starting point) was selected purposively (applying wisdom by looking at the surrounding species composition and terrain position) so that it became representative of the surrounding woody species. From the plot centre, 4 transects of each 15 meters length were laid out in four sides, perpendicular to each other, using measuring tape (fig 2.3). Woody species composition was recorded at each 2.5 m distance of each transects from the plot centre till 15 meter was reached. Therefore each plot covered maximum plot size of 30m×30m which conforms to standard forest inventory (e.g $20m^2$; Kangas and Maltamo, 2007). This strategy of data collection is very useful for training differential spatial resolution satellite data with the species composition of different plot size corresponding to their spatial resolution (for ALOS and TM, 10m and 30m respectively) without resampling the imageries to a common spatial resolution (equal to the field plot) for comparison.

Woody species which had significant contribution in the canopy (and ultimately to canopy reflectance recorded in the satellite sensor) were recorded. Nomenclature of the trees was done following Conti (1998). Topographical map (available in Majella), compass and iPAQ were used to navigate to each sample plot in the field. Coordinate of the center of each plot was recorded using iPAQ and Garmin 12 channel GPS (Global Positioning System). Spatial accuracy of both the GPSs was 1-5m (experienced in the field).

2.3.5 Field data processing

Several measures/indices of diversity are used to describe complexity of a biological community. A species diversity index can condense extensive amounts of data available on the abundance of numerous species to a single, quantitative expression (Sager and Hasler, 1969). Shannon indices (Shannon, 1948) have been used in this research as indicator of woody species diversity as they are the most commonly used and acceptable indicator of biodiversity (Mouillot, D., Leprêtre, A. 1999; Kent and Coker, 1992). Shannon diversity index (H) (for comprehensive details, readers are referred to Magurran, 1988) has been used as a measure of species richness and abundance (Onaindia et al., 2004), while Shannon Evenness index-SEI (E) has been used as an indicator of relative abundance or equitability (Izsa´k, 2007) of woody species in the study area.

Formula used for Shannon diversity index (H) = $-\sum_{1}^{S} P_i \ln P_i$

Here P_i is the proportion of total number of species made up of the *i* th species in the plot where S refers to the total number of species or species richness (also called α diversity) of that particular plot (Whittaker, 1972; Pielou, 1975).

Formula for calculating Shannon evenness index (E) = H / log(S).

Shannon diversity and evenness indices were calculated for each of the 100 field sample plots independently using the above mentioned formulae. TM image posses 30m×30m spatial resolution; therefore for classification of TM data, Shannon diversity (H) and Evenness (E) indices were calculated using the ground sample plot species composition of 30m×30m size from plot centre (i.e. the whole sample plot data). On the other hand ALOS image posses 10m spatial resolution; therefore for classifying ALOS data, Shannon diversity (H) and Evenness (E) indices were calculated using the ground sample plot species composition of 10m1×0m size from plot centre. This approach is feasible as well as necessary to train the image classifier keeping the image spatial resolution intact because, in this case, no re-sampling of the imageries to a common spatial resolution is required for classification accuracy comparison between the two.

Shannon diversity and evenness indices of the 100 sample plot transects were then ranked to 5 discrete diversity and evenness classes (e.g. Gillespie et al., 2008; Cayuela et al., 2006; Hurlbert and White, 2005; Gould, 2000; Harrison, 1992). The classes are: very low, low, medium, high and very high. Calculated diversity and evenness indices were ordered separately in descending order (smaller to larger) in MS Excel followed by categorization to 5 equidistant classes; thus each class contains indices value of 20 sample plots. The lowest value for both Shannon diversity and evenness indices are zero indicating only one species present in those plots.

2.3.6 Image classification

Backpropagation Neural Network has been used to classify imageries, which has been successfully used by some researchers (e.g. Mutanga and Kumar, 2007; Skidmore et al., 1997). All the environmental data layers (elevation, slope, aspect and solar radiation) were stacked together with the satellite imageries while they were fed up to the NN classifier in ENVI 4.3. The Classifier was run with different possible combinations (16) of environmental layers and imageries. Each time run of NN provides output as respective diversity or evenness map.

70% of the field sample data (i.e. 14 plots out of 20) was used as training dataset and 30% of the field plots data (i.e. 6 out of 20) was used as validation data set, which was randomly selected using Hawths tool in ArcGIS 9.3. In fact, this proportion is recommended in different publications (e.g Mutanga and Rugege, 2006; Skidmore, 1999; Mcgarigal et al., 2000) as it gives more weight to data for model build-up.

2.3.7 Multicollinearity test

Multicollinearity implies a phenomenon where there exists a high degree of correlation amongst two or more explanatory variables in a regression model and difficult to separate their individual effect on the dependent variable (see explanations in Dirk and Bart, 2004). Multicollinearity occurs when independent variables are so highly correlated to each other that both actually measure the same thing. Multicollinearity is a statistical parameter and assessed by examining two diagnostic factors; tolerance and Variance Inflation Factor (VIF), which are reciprocally related as follows:

Tolerance = 1-R^2, VIF =1/tolerance

Both tolerance and VIF are widely used, reasonable and intuitive measure of multicollinearity (O'brien, 2007) and are calculated by common statistical programmes, for example SPSS. There is no formal VIF value to determine multicollinearity among variables but several rules of thumb exist, such as rule of 4, rule of 5, rule of 10 or 30 etc. Some authors noted VIF less than 5 is a cause of concern (e.g. Menard, 1965); some others reported VIF greater than 10 is a serious concern (e.g. Mason et al., 1989) or indicate high multicollinearity (e.g. Hair et al., 1995; Kennedy, 1992; Marquardt, 1970). Of course, among all of the rules, rule of 10 is the most common (O'brien, 2007); stating that a VIF greater than 10 indicates evidence of multicollinearity among the independent variables.

When VIF value reaches to the threshold, one or more independent variables that are highly related to other independent variables are removed from the analysis and the model is run with the remaining variables (O'brien, 2007; Chatterjee and Price, 1991).

We extracted respective pixel values of all the input layers including all bands of imageries, corresponding to 100 field sample plots, using 'Extract values to sample' tool in ArcGIS 9.3. Then we calculated VIF value of the independent variable layers such as among all the bands of TM (6 bands) and ALOS (4 bands) imageries and other ancillary environmental data layers (4 layers) namely elevation, slope, aspect and solar radiation using SPSS statistical software (see details in the result and discussion chapters). Independent layers which showed VIF value greater than 10 were excluded in the process of elimination, and layers which showed VIF value less than 10 were included for subsequent use in NN for classification (Appendix 1 and 2).

2.3.8 Image band number and mapping accuracy

We used 6 bands for TM (bands 1 to 5 and 7) and 4 bands for ALOS imageries along with other ancillary environmental data in the NN for mapping species diversity. Interestingly, first 4 bands of TM overlaps with 4 bands of ALOS imagery (Table 2.4) with very subtle difference. To investigate why one image maps woody species diversity more accurately than the other, we made the proposition that the cause might be due to more number of bands present in one image than another.

Aiming to that, image classification in NN was run with overlapping first 4 bands of TM to compare the accuracy against ALOS. The whole process was replicated with all possible layer combinations similar to that used for all the bands and other environmental layers (as previously mentioned).

Table 2.4: Band overlaps (in µm) of TM and ALOS.

Band	TM	ALOS
1	0.450-0.520	0.42-0.50
2	0.520-0.600	0.52-0.60
3	0.630-0.690	0.61-0.69
4	0.760-0.900	0.76-0.89
5	1.550-1.750	n/a
7	2.080-2.350	n/a

Note: Band 6 has not been used

2.3.9 Map accuracy assessment

Maps and images are inherently erroneous (Skidmore, 1999). Therefore, accuracy assessment is a fundamental exercise in mapping practice and a major priority area of research (Rindfuss et al., 2004). Classified maps are hardly used without assessment of their accuracy as quality of the classified maps depends on their classification accuracy (Foody, 2002). Although there is no standard method of accuracy assessment, confusion matrix (also known as error matrix) is the basis of quantitative matrices of classification accuracy assessment (Foody, 2002; Congalton, 1991) and most widely used unquestionably to its suitability (Foody, 2002). Despite many problems of the current status of accuracy assessment remaining unsolved (Foody, 2002) and having no decisive flawless method of accuracy assessment of classified image, we, in this report, calculated the confusion matrix for each of the classification results as it is an acceptable and widely used approach. The process involved using the independent ground validation data against each of the classification result from NN (using ENVI 4.3 software's post classification confusion matrix option) where the outputs were generated as confusion matrices with overall, user's, producer's accuracies and Kappa statistic (Congalton and Green, 1999; Cohen, 1960).

2.3.10 Statistical significance test of the map accuracy

After generating the confusion matrix in the process of accuracy assessment, it is need to know whether the classification results (or confusion matrices) were significantly different from each other. Let us say, one image classification with two associated environmental layers resulted with Kappa 0.58 while same image classification with three associated environmental layers results with Kappa 0.68. We need to know whether second classification result is significantly different from the first one. Therefore to ascertain if any two classification results are significantly different, we used the method described by Cohen (1960), and elaborated by various authors (e.g. Rossiter, 2004; Skidmore, 1999; Congalton et al., 1983). This method uses the normal curve deviate statistic (z) and the Kappa values (k_1, k_2) and their associated variance ($\sigma^2_{[k1]}$, $\sigma^2_{[k2]}$) as follows:

$$Z = \frac{K_1 - K_2}{\sqrt{\sigma^2[K_1] + \sigma^2[K_2]}}$$

At 95% level of significance (α= 0.05), the tabulated value of z is 1.96 (z=1.96). If the calculated value of z is less than the tabulated value, there is no significant difference between two classification results. If the calculated value is greater than the tabulated value, there is significant difference between two classifications. Z value was calculated for all the possible paired combinations of independent error matrices.

2.3.11 Overlapping forest types map with diversity and evenness maps

Widely used forest types map of Majella was overlapped with the diversity and evenness maps separately using ArcGIS 9.3 to see the agreement of diversity and evenness information between them. Average value of Shannon diversity (H) and evenness (E) indices of field samples falling in each forest types was compared with the remotely sensed level/class of diversity and evenness of each forest type.

Chapter 3: Results

3.1 Mapping woody species diversity

3.1.1 Mapping woody species diversity by using TM and ALOS

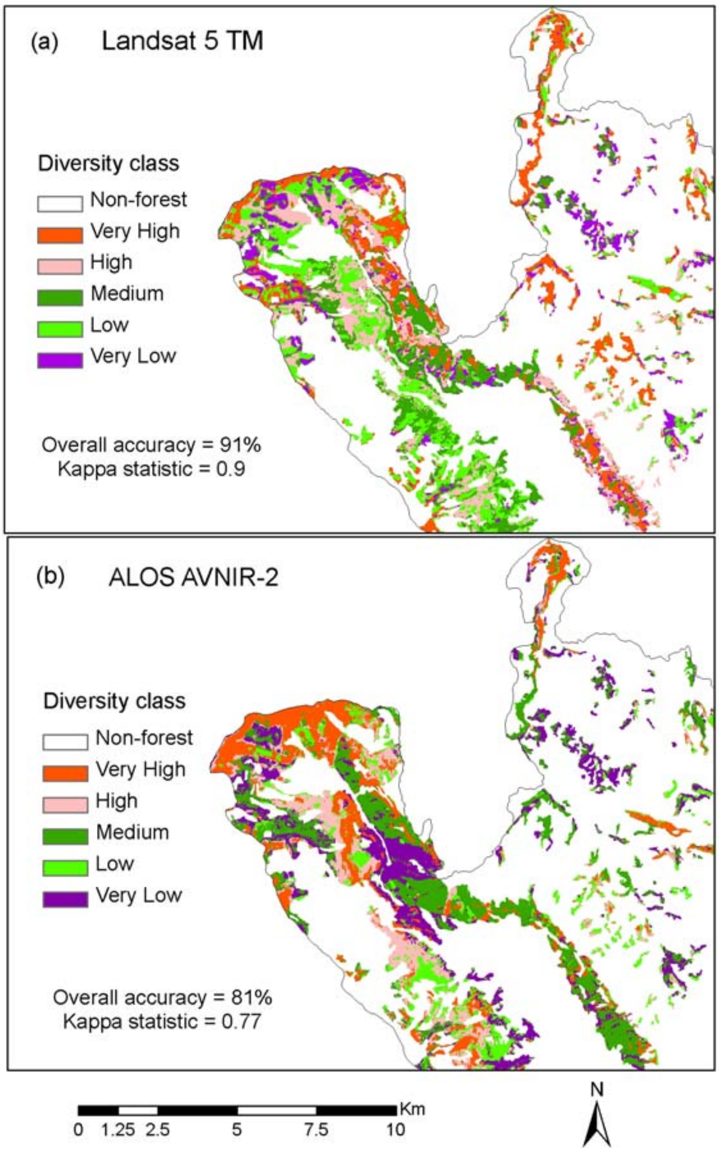

Fig 3.1: Neural Network classification result for Shannon diversity index (H). (a) Classified TM image (b) Classified ALOS image

Woody species diversity of Majella was mapped by using all the bands of TM and ALOS satellite imageries independently using other ancillary environmental data (elevation, slope, aspect and solar radiation) with NN classifier. Shannon diversity index (H) was used as a surrogate measure of woody species diversity in five diversity levels/classes; very high, high, medium, low and very low. Fig 3.1 represents the two classified imageries with five diversity classes.

TM imagery maps woody species diversity of study site with an overall accuracy of 91% and Kappa statistic 0.9. On the other hand ALOS imagery mapped woody species diversity with 81% overall accuracy and 0.77 associated Kappa statistic. Evidently the overall mapping accuracy of woody species diversity by TM image is 10% higher than that obtained by using ALOS imagery.

3.1.2 Accuracy assessment

Table 3.1 and 3.2 show two of the confusion matrices, from among different others layer combinations, with highest level of overall accuracy of TM (91%) and ALOS (81%) imageries respectively using all the input layers (all bands of both imageries +4 environmental layers).

Table 3.1: Accuracy assessment of woody species diversity map produced by using TM with NN classifier, with Kappa statistic, Overall Accuracy (OA), Omission Error (OE), Producer Accuracy (PA), Commission Error (CE) and User Accuracy (UA).

	High	Low	Medium	Very High	Very Low	CE%	UA%
High	14	1	1	0	2	22	78
Low	0	13	1	0	0	7	93
Medium	0	0	12	0	1	8	92
Very High	0	0	0	14	0	0	100
Very Low	0	0	0	0	11	0	100
OE%	0	7	14	0	21		
PA%	100	93	86	100	79		

Overall Accuracy=91.43% Kappa Statistic= 0.89

The main confusion for TM imagery case is that *High* diversity class has been mapped as *Very Low* (Table 3.1). In case of ALOS, the main confusions were *Very High* diversity level has been mapped as *Very Low* while *Low* has been mapped as *Medium* (Table 3.2)

Table 3.2: Accuracy assessment of woody species diversity map produced by using ALOS with NN classifier, with Kappa statistic, Overall Accuracy (OA), Omission Error (OE), Producer Accuracy (PA), Commission Error (CE) and User Accuracy (UA).

	High	Low	Medium	Very High	Very Low	CE%	UA%
High	11	0	1	0	0	8	92
Low	1	11	2	1	1	31	69
Medium	1	1	11	0	0	15	85
Very High	1	0	0	11	0	8	92
Very Low	0	2	0	2	13	24	76
OE%	21	21	21	21	7		
PA%	79	79	79	79	93		

Overall Accuracy=81.43, Kappa Statistic=0.77

Four ancillary environmental data layers namely elevation, aspect, slope and solar radiation were used along with the satellite imageries with 16 different possible combinations to run in the NN classifier. All the possible combinations with their respective overall mapping accuracy and Kappa statistic have been presented in table 3.3.

Table 3.3: Mapping accuracy of Shannon diversity index by TM and ALOS, ordered by Overall Accuracy (OA%) of TM image. Significantly different paired layer combinations with 95% confidence ($z \geq 1.96$) are boldfaced.

		OA %		Kappa		z
		TM	ALOS	TM	ALOS	
1.	IMAGE+ASPECT+DEM+SLOPE+ S.RADIATION	91	81	0.89	0.77	**2.19**
2.	IMAGE+ASPECT+DEM+SLOPE	87	80	0.84	0.75	1.43
3.	IMAGE+SLOPE	86	64	0.82	0.55	**3.80**
4.	IMAGE+DEM+SLOPE+S. RADIATION	86	79	0.82	0.73	1.39
5.	IMAGE+SOLAR ADIATION+DEM	84	74	0.80	0.68	1.85
6.	IMAGE+SOLAR ADIATION+SLOPE	83	73	0.79	0.66	1.80
7.	IMAGE+DEM+ASPECT+S.RADIATION	83	76	0.79	0.70	1.31
8.	IMAGE+ASPECT + DEM	81	74	0.77	0.68	1.28
9.	IMAGE+SLOPE+ASPECT+S. RADIATION	81	80	0.77	0.75	0.27
10.	IMAGE+DEM+SLOPE	80	77	0.75	0.71	0.52
11.	IMAGE+ASPECT+SLOPE	80	74	0.75	0.68	1.01
12.	IMAGE+SOLAR ADIATION+ASPECT	77	70	0.71	0.63	1.21
13.	IMAGE+SOLAR RADIATION	70	69	0.63	0.61	0.23
14.	IMAGE+ASPECT	67	69	0.59	0.61	0.23
15.	IMAGE+DEM	66	67	0.57	0.59	0.22
16.	IMAGE	60	53	0.50	0.41	1.08

As noticeable from the Table 3.3, TM imagery maps woody species diversity more accurately than ALOS imagery with or without the use of environmental data layers in NN. For nearly all of the environmental layer combinations as well as in the case of using only the image, TM mapping accuracy (and associated Kappa statistic) is higher than that of ALOS. But for most of the paired layer combinations, the accuracy difference is not significant except for a few cases e. g. highest accuracy obtained by using all layers (z = 2.19) and by using image with slope (IMAGE+SLOPE, z score 3.80). From this observation, we generalize the fact that TM data is better in mapping woody species diversity than ALOS data.

3.1.3 Effect of incorporating environmental layers on mapping accuracy

Mapping accuracy of woody species diversity increases significantly if environmental layers are used along with both imageries. As an example, the overall mapping accuracy obtained by using only TM image in the NN produces 60% overall accuracy (with Kappa 0.5); but when the image was used with four other GIS layers namely elevation, aspect, slope and solar radiation, the overall mapping accuracy rises to 91% (with Kappa 0.89). Similarly, ALOS imagery when used alone in the NN, maps the species diversity with 53% overall accuracy (and Kappa 0.41); on the other hand imagery used with four environmental layers namely aspect, DEM, slope and solar radiation, the overall accuracy rises to 81% (with Kappa 0.77) (Table 3.3). For any other combination of the input environmental layers, mapping accuracy is higher than that obtained by using the image alone (Table3.3). This trend is true for both TM and ALOS imagery cases.

3.1.4 Statistical comparison of the accuracy assessment

Statistical comparison of the confusion matrices that resulted from the accuracy assessment against outputs of NN classification by field validation data was done using the z statistic (Cohen, 1960) and has been presented in the following tables; for TM (Table 3.4) and for ALOS (Table 3.5). Significantly different layer combinations have been boldfaced. As for example, the z value of the statistical comparison of layer pairs 14 (IMAGE+DEM) and 16 (IMAGE) in Table 3.5 is 2.21 which is greater than critical value of z (1.96); therefore it has been boldfaced. This simply means that the accuracy obtained by using ALOS image and DEM together in NN is significantly higher than the accuracy obtained by using ALOS image only. In combination with TM image, slope comes with highest accuracy (86%) followed by solar radiation (70%), aspect (67%) and elevation (66%). For ALOS, solar radiation and aspect produces same accuracy (69%) which is the highest, followed by elevation (67%) and slope (64%).

Table 3.4: Statistical comparison of the accuracy assessments of Shannon Diversity Index (H) of TM ordered by Overall Accuracy (OA%) using the *z*-statistic. Significantly different layer pair combinations with 95% confidence ($z \geq 1.96$) are boldfaced.

		1	2	3	4	5	6	7	8	9	10	11	12	13	14	15	OA%	Ka
1.	IMAGE+ASPECT+DEM+SLOPE+SOLAR RADIATION																81	0.77
2.	IMAGE+ASPECT+DEM+SLOPE	0.27															80	0.75
3.	IMAGE+SLOPE+ASPECT+SOLAR RADIATION	0.27	0.00														80	0.75
4.	IMAGE+DEM+SLOPE+SOLAR RADIATION	0.53	0.26	0.26													79	0.73
5.	IMAGE+DEM+SLOPE	0.78	0.52	0.52	0.26												77	0.71
6.	IMAGE+ASPECT+DEM+SOLAR RADIATION	1.03	0.77	0.77	0.51	0.25											76	0.70
7.	IMAGE+SOLAR ADIATION+DEM	1.28	1.01	1.01	0.75	0.49	0.00										74	0.68
8.	IMAGE+ASPECT+DEM	1.28	1.01	1.01	0.75	0.49	0.24	0.00									74	0.68
9.	IMAGE+ASPECT+SLOPE	1.28	1.01	1.01	0.75	0.49	0.24	0.00	0.00								74	0.68
10.	IMAGE+SOLAR ADIATION+SLOPE	1.52	1.25	1.25	0.99	0.73	0.48	0.24	0.24	0.24							73	0.66
11.	IMAGE+SOLAR ADIATION+ASPECT	**2.00**	1.73	1.73	1.46	1.21	0.96	0.71	0.71	0.71	0.47						70	0.63
12.	IMAGE+SOLAR RADIATION	**2.22**	1.95	1.95	1.69	1.43	1.18	0.94	0.94	0.94	0.70	0.23					69	0.61
13.	IMAGE+ASPECT	**2.22**	1.95	1.95	1.69	1.43	1.18	0.94	0.94	0.94	0.70	0.23	0.00				69	0.61
14.	IMAGE+DEM	**2.46**	**2.19**	**2.19**	1.93	1.67	1.42	1.17	1.17	1.17	0.93	0.46	0.23	0.23			67	0.59
15.	IMAGE+SLOPE	**2.92**	**2.65**	**2.65**	**2.39**	**2.12**	1.87	1.62	1.62	1.62	1.38	0.91	0.67	0.67	0.45		64	0.55
16.	IMAGE	**4.78**	**4.49**	**4.49**	**4.22**	**3.94**	**3.68**	**3.41**	**3.41**	**3.41**	**3.16**	**2.68**	**2.44**	**2.43**	**2.21**	1.75	53	0.41

Table 3.5: Statistical comparison of the accuracy assessments of Shannon Diversity Index (H) of ALOS ordered by Overall Accuracy (OA %) using the *z*-statistic. Significantly different layer pair combinations with 95% confidence ($z \geq 1.96$) are boldfaced

		1	2	3	4	5	6	7	8	9	10	11	12	13	14	15	OA%	Ka
1.	IMAGE+ASPECT+DEM+SLOPE+SOLAR RADIATION																91	0.89
2.	IMAGE+ASPECT+DEM+SLOPE	1.03															87	0.84
3.	IMAGE + SLOPE	1.34	0.31														86	0.82
4.	IMAGE+DEM+SLOPE+SOLAR RADIATION	1.34	0.31	0.00													86	0.82
5.	IMAGE+SOLAR RADIATION+DEM	1.63	0.61	0.30	0.30												84	0.80
6.	IMAGE+ASPECT+DEM+SOLAR RADIATION	1.91	0.89	0.58	0.58	0.29											83	0.79
7.	IMAGE+SOLAR ADIATION+SLOPE	1.91	0.89	0.58	0.58	0.29	0.00										83	0.79
8.	IMAGE+SLOPE+ASPECT+SOLAR RADIATION	**2.19**	1.17	0.86	0.86	0.56	0.28	0.28									81	0.77
9.	IMAGE+ASPECT+DEM	**2.19**	1.17	0.86	0.86	0.56	0.28	0.28	0.00								81	0.77
10.	IMAGE+DEM+SLOPE	**2.45**	1.44	1.13	1.13	0.83	0.55	0.55	0.00	0.00							80	0.75
11.	IMAGE+ASPECT+SLOPE	**2.45**	1.44	1.13	1.13	0.83	0.55	0.55	0.27	0.27	0.00						80	0.75
12.	IMAGE+SOLAR ADIATION+ASPECT	**2.97**	**1.95**	1.35	1.35	1.35	1.06	1.06	0.78	0.78	0.52	0.52					77	0.71
13.	IMAGE+SOLAR RADIATION	**4.20**	**3.18**	**2.57**	**2.57**	**2.57**	**2.28**	**2.28**	**2.00**	**2.00**	1.73	1.73	1.21				70	0.63
14.	IMAGE+ASPECT	**4.69**	**3.66**	**3.04**	**3.04**	**3.04**	**2.75**	**2.75**	**2.47**	**2.47**	**2.20**	**2.20**	1.67	0.46			67	0.59
15.	IMAGE+DEM	**4.89**	**3.87**	**3.56**	**3.56**	**3.26**	**2.97**	**2.97**	**2.69**	**2.69**	**2.41**	**2.41**	1.89	0.68	0.23		66	0.57
16.	IMAGE	**5.87**	**4.82**	**4.50**	**4.50**	**4.19**	**3.90**	**3.90**	**3.61**	**3.61**	**3.33**	**3.33**	**2.80**	1.57	1.11	0.88	60	0.50

3.1.5 Multicollinearity test

Multicollinearity was assessed by calculating Variance Inflation Factor (VIF) among the input layers of NN to determine redundancy. Input layers which showed VIF value greater than 10 were screened out. Some of the bands of both ALOS and TM imageries were found to be multicollineared. For TM imagery, bands TM 3 and TM 5 were found having the problem of multicollinearity with VIF value greater than 10; therefore excluded from the analysis. Only bands TM 1, TM 2, TM 4 and TM 6 were included in NN (Appendix 1). For the case of ALOS data, band no 3 showed VIF value greater than 10; therefore excluded from classification in NN. Only bands 1, 2 and 4 of did not show multicollinearity; therefore these three bands were included in subsequent analysis (Appendix 2). On the other hand none of the environmental layers showed multicollinearity with respective VIF value less than 10 as a rule of thumb (Appendix 1 and 2). Appendix 3 shows the overall accuracy and Kappa statistic of the accuracy assessment of the NN outputs with layers that do not have the problem of multicollinearity Values of Kappa and overall accuracy of the respective NN outputs using all the available bands of both of the imageries are also presented in the Appendix 3, side by side for easy comparison.

As noticed from the Appendix 3, the overall accuracy of produced map by using layers without multicollinearity declines than that obtained by using all the 6 bands of TM without considering multicollinearity; but the amount of drop is not significant and the values are very near to each other in almost all the layer combinations. Highest accuracy drops from 91% to 87%. The same trend is true for the ALOS. The highest accuracy obtained by using bands with multicollinearity and without multicollinearity is just 81% and 80% respectively. That is to say, multicollinearity among some of the bands of TM and ALOS imageries does not affect the overall mapping accuracy significantly.

3.1.6 Effect of image number of bands on mapping accuracy

In quest of why ALOS maps woody species diversity less accurately than TM and if the matter is due to the fact that TM has more bands than ALOS, we run the neural NN with the first 4 overlapping bands (see Table 2.4) of TM with ALOS with other ancillary environmental data. Overall accuracy and Kappa coefficient of the accuracy assessment of the results obtained by NN classification is presented in the Appendix 4. For easy comparison, the accuracy obtained by using 6 bands and 4 bands of TM and all 4 bands of ALOS, they are presented side by side (Appendix 4).

Overall accuracy attained by using 4 bands of TM drops or remains equal than that by using 6 bands, for majority of the combinations. Highest accuracy falls from 91% to 84% (combination 1) while lowest falls from 60% to 53% (combination 16).

But the difference in accuracy is insignificant in most of the cases (as such combinations 3, 7, 8), and significant in very few cases (e.g. combination 11) or in some cases equal (as such combination 4, 15).

The overall accuracy obtained by using 4 bands of TM in all the layer combinations are greater than ALOS, except combination no 15 (Image + Aspect), where ALOS accuracy is a little higher (69%) than TM (67%). Of course the difference in accuracy between corresponding layer combinations of 4 bands of TM and ALOS are not significant (as such combination 2, 4, 6) or the accuracy is the same (as such combination 7, 16). As for example, the highest accuracy obtained by 4 bands of TM and ALOS with all the input layers are 84% and 81% respectively; where the overall accuracy difference is only 3%, which is not significant.

3.1.7 Overlapping forest type map of Majella with diversity map

The forest type map of Majella was overlapped with the produced maps of species diversity in NN, as an extra check for the assessment of accuracy.

Table 3.6: Result of overlapping TM highest accuracy diversity map with forest types map of Majella along with average values of Shannon Diversity Index (SDI) in each forest type. Major diversity level in each forest type has been boldfaced.

Forest types	Diversity Class (%) Very High	High	Medium	Low	Very Low	SDI* (avg)
Beech	20	26	**34**	11	9	0.65^{M}
Black/Aleppo Pine	8	22	27	**34**	9	0.82^{M}
Evergreen Oak	27	9	4	**39**	21	0.52^{L}
Hop-hornbeam	14	**32**	17	29	8	1.14^{VH}
Deciduous Oak	**34**	17	14	17	18	0.72^{H}

SDI*= average value of Shannon Diversity Index in each forest types; Diversity classes, M=Medium; L=Low; H=High; VH= Very High

Table 3.6 shows the result of overlap of forest type map with TM diversity map having highest accuracy (91%). Major diversity class in each forest type has been boldfaced. There is good agreement between the average value of SDI in each forest type with the majority portion of that forest type belonging to the respective or nearby diversity map classes. For example, average value of SDI of beech forest is 0.65 which falls within the range of *Medium* diversity class, while majority proportion of beech forest (34%) also belongs to *Medium* diversity class. In other forest types also fair agreement exist between average value of SDI with majority area of each forest types belonging to identical or nearby diversity class.

3.2 Mapping woody species evenness

3.2.1 Mapping woody species evenness by using TM and ALOS

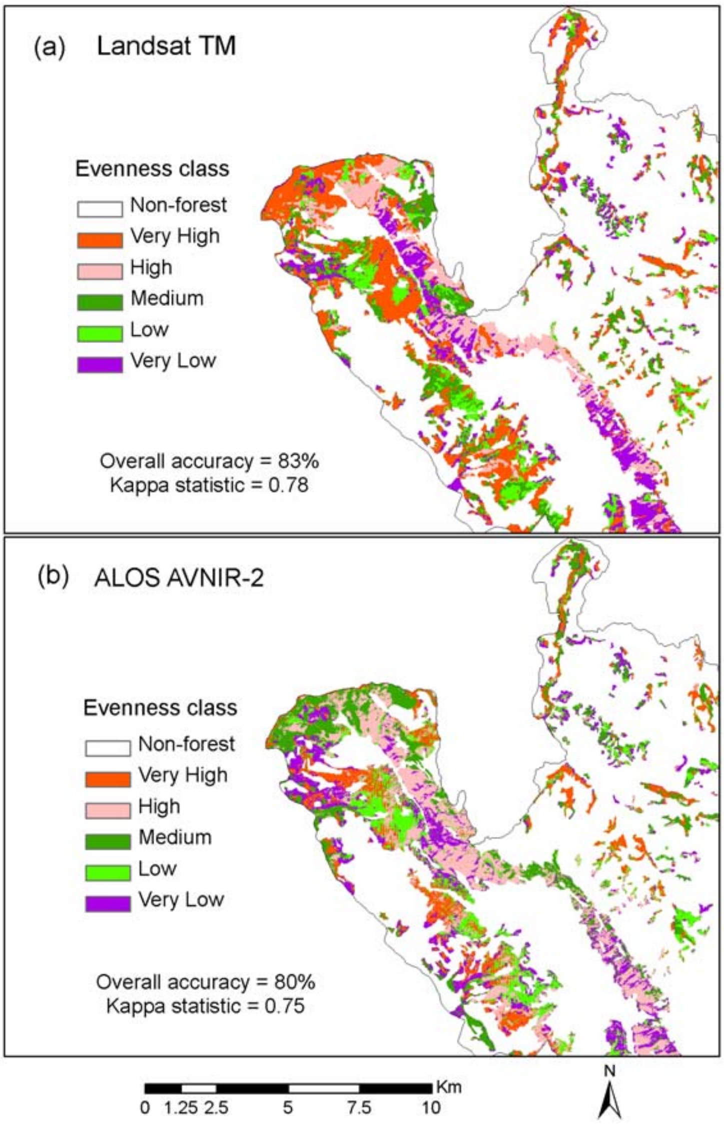

Fig 3.2: Neural network classification result for Shannon evenness index (E). (a) Classified TM image (b) Classified ALOS image

Woody species evenness of the study site was mapped by using all bands of TM and ALOS satellite imageries and ancillary environmental data (elevation, slope, aspect and solar radiation) with NN classifier. Shannon evenness index (E) was used to obtain five evenness levels/classes; very high, high, medium, low and very low. Classified imageries with five evenness classes have been shown in Fig3.2.

TM imagery maps woody species evenness with an overall accuracy of 83% and Kappa statistic 0.78. On the other hand ALOS imagery mapped woody species diversity with 80% overall accuracy and 0.75 associated Kappa statistic. Evidently the overall mapping accuracy of woody species diversity by TM image is 3% higher than that obtained by using ALOS imagery.

3.2.2 Accuracy assessment

Table 3.7 and 3.8 show two of the confusion matrices, from among different others layer combinations, with highest level of overall accuracy of TM (83%) and ALOS (80%) imageries respectively using all the input layer (all bands of both imageries+4 environmental layers).

The main confusions for TM confusion matrix are that *High* evenness class has been mapped as *Low* and *Medium* as *High* (Table 3.7). In case of ALOS, the main confusions were, *High* evenness class has been mapped as *Low*, *Low* as *High* and *Medium* as *Very Low* (Table 3.8). Some of the classes e.g. *Very Low* has been classified with high accuracy in both of the image matrices.

Table 3.7: Accuracy assessment of woody species evenness map produced by using TM imagery with neural network classifier, with Kappa statistic, Overall Accuracy (OA), Omission Error (OE), Producer Accuracy (PA), Commission Error (CE) and User Accuracy (UA).

	High	Low	Medium	Very High	Very Low	CE%	UA%
High	11	2	0	1	1	27	73
Low	0	10	0	0	0	0	100
Medium	2	1	13	1	1	28	72
Very High	1	1	0	12	0	14	86
Very Low	0	0	1	0	12	8	92
OE%	21	29	7	14	14		
PA%	79	71	93	86	86		

Overall Accuracy = 83%, Kappa Statistic = 0.79

Table 3.8: Accuracy assessment of woody species evenness map produced by using ALOS imagery with neural network classifier, with Kappa statistic, Overall Accuracy (OA), Omission Error (OE), Producer Accuracy (PA), Commission Error (CE) and User Accuracy (UA).

	High	Low	Medium	Very High	Very Low	CE%	UA%
High	11	2	1	1	0	27	73
Low	2	11	0	0	1	21	79
Medium	0	1	12	1	2	25	75
Very High	1	0	1	11	0	15	85
Very Low	0	0	0	1	11	8	92
OE%	21	21	14	21	21		
PA%	79	79	86	79	79		

Overall Accuracy = 80%, Kappa Statistic = 0.75

Four ancillary environmental data layers namely elevation, aspect, slope and solar radiation were used along with the satellite imageries with 16 different possible combinations with the imageries in the NN classifier. All the possible combinations with their respective overall mapping accuracy and Kappa statistic have been presented in Table 3.9. Significantly different layer combinations with 95% level of confidence ($z \geq 1.96$) have been boldfaced

As we compare the overall accuracies (or Kappa statistic) achieved for the produced woody species evenness maps presented in Table 3.9) by using TM and ALOS imageries, overall accuracy of TM is greater than ALOS for majority of the layer combinations. Statistically significant ($z \geq 1.96$) layer pairs between imageries are boldfaced. In some combinations, TM accuracies are significantly higher than ALOS. (E.g. layer combinations 9, 14 and 16). The higher accuracy obtained for TM is 83% while for ALOS it is 80%. Lowest accuracy for TM is 59% while for ALOS is 46%. This trend is true for all of the input layer combinations in NN classifier, although the differences in mapping accuracies of the two imageries are not significant for most of the combinations. Therefore, evidently, TM maps woody species evenness more accurately than ALOS.

3.2.3 Effect of incorporating environmental layers on accuracy

Accuracy of the produced species evenness map increases tremendously when ancillary GIS layers are used in association with both the imageries in the NN. In some cases, the overall accuracy nearly doubled when GIS layers were jointly used with the images as such 46% overall accuracy was achieved using only ALOS image but when ALOS was associated with all other ancillary environmental data in

NN, the overall accuracy jumped up to 80% (Table 3.9). Lowest map accuracies obtained by using only imageries were 59% and 46% respectively for TM and ALOS and by using all ancillary environmental data jointly with imageries, highest accuracies were 83% and 80% respectively. Ancillary environmental data enhances the mapping accuracy of woody species evenness significantly when jointly used with satellite data.

Table 3.9: Mapping accuracy comparison of Shannon evenness index by TM and ALOS imagery, ordered by Overall Accuracy (OA%) of TM image. Significantly different layer pairs with 95% confidence ($z \geq 1.96$) are boldfaced.

	OA%		Kappa		z
	TM	ALOS	TM	ALOS	
1. IMAGE+ASPECT+DEM+SLOPE+ S.RADIATION	83	80	0.79	0.75	0.54
2. IMAGE+ASPECT+DEM+SLOPE	81	74	0.77	0.68	1.28
3. IMAGE+SLOPE+ASPECT+S. RADIATION	81	76	0.77	0.70	1.03
4. IMAGE+ASPECT+DEM	79	67	0.73	0.59	1.92
5. IMAGE+SOLAR ADIATION+DEM	79	76	0.73	0.70	0.51
6. IMAGE+SOLAR RDIATION+SLOPE	79	69	0.73	0.61	1.70
7. IMAGE+DEM+SLOPE	79	69	0.73	0.61	1.69
8. IMAGE+DEM+SLOPE+S. RADIATION	79	71	0.73	0.64	1.23
9. IMAGE+SOLAR ADIATION+ASPECT	77	63	0.71	0.54	**2.34**
10. IMAGE+DEM+ASPECT+S. RADIATION	77	77	0.71	0.71	0.00
11. IMAGE+SLOPE	73	63	0.66	0.54	1.60
12. IMAGE+ASPECT+SLOPE	73	71	0.66	0.64	0.24
13. IMAGE+ASPECT	71	61	0.64	0.52	1.58
14. IMAGE+DEM	70	54	0.63	0.43	**2.44**
15. IMAGE+SOLAR RADIATION	69	67	0.61	0.59	0.23
16. IMAGE	59	46	0.48	0.32	**1.97**

3.2.4 Statistical comparison of the accuracy assessment

Table 3.10 and 3.11 includes the result of the statistical comparison of the accuracy assessments of Shannon Evenness Index (E) of TM and ALOS respectively. The study used the *z*-statistic as a measure for the estimation of statistical significance among different layer combinations where significantly different layer pairs with 95% confidence ($z \geq 1.96$) have been boldfaced. In combination with the image, slope showed the highest accuracy (73%), followed by aspect (71%), elevation (70%) and solar radiation (69%). In case of ALOS, solar radiation and slope provided same highest accuracy (63%), followed by aspect (61%) and elevation (54%). Thus, individual effect of the layers on accuracy is not prominently different than each other.

Table 3.10: Statistical comparison of the accuracy assessments of Shannon Evenness Index (E) of TM ordered by Overall Accuracy (OA %) using the *z*-statistic. Significantly different layer pairs with 95% confidence (z ≥ 1.96) are boldfaced.

		1	2	3	4	5	6	7	8	9	10	11	12	13	14	15	OA%	Ka
1.	IMAGE+ASPECT+DEM+SLOPE+SOLAR RADIATION																83	0.79
2.	IMAGE+ASPECT+DEM+SLOPE	0.28															81	0.77
3.	IMAGE+SLOPE+ASPECT+SOLAR RADIATION	0.28	0.00														81	0.77
4.	IMAGE+ASPECT+DEM	0.80	0.53	0.53													79	0.73
5.	IMAGE+SOLAR ADIATION+DEM	0.80	0.53	0.53	0.00												79	0.73
6.	IMAGE+SOLAR RDIATION+SLOPE	0.80	0.53	0.53	0.00	0.00											79	0.73
7.	IMAGE+DEM+SLOPE	0.80	0.53	0.53	0.00	0.00	0.00										79	0.73
8.	IMAGE+DEM+SLOPE+SOLAR RADIATION	0.80	0.53	0.53	0.00	0.00	0.00	0.00									79	0.73
9.	IMAGE+SOLAR ADIATION+ASPECT	1.06	0.78	0.78	0.25	0.25	0.25	0.25	0.25								77	0.71
10.	IMAGE+ASPECT+DEM+SOLAR RADIATION	1.06	0.78	0.78	0.00	0.00	0.00	0.00	0.00	0.00							77	0.71
11.	IMAGE+SLOPE	1.80	1.52	1.52	0.73	0.73	0.73	0.73	0.73	0.73	0.73						73	0.66
12.	IMAGE+ASPECT+SLOPE	1.80	1.52	1.52	0.73	0.73	0.73	0.73	0.73	0.73	0.73	0.00					73	0.66
13.	IMAGE+ASPECT	**2.04**	1.76	1.76	0.97	0.97	0.97	0.97	0.97	0.97	0.97	0.24	0.24				71	0.64
14.	IMAGE+DEM	**2.27**	**1.99**	**1.99**	1.20	1.20	1.20	1.20	1.20	1.20	1.20	0.47	0.47	0.23			70	0.63
15.	IMAGE+SOLAR RADIATION	**2.52**	**2.23**	**2.23**	1.44	1.44	1.44	1.44	1.44	1.44	1.44	0.70	0.70	0.46	0.23		69	0.61
16.	IMAGE	**4.18**	**3.89**	**3.89**	**3.32**	**3.32**	**3.32**	**3.32**	**3.32**	**3.06**	**3.06**	**2.29**	**2.29**	**2.05**	1.81	1.58	59	0.48

Table 3.11: Statistical comparison of the accuracy assessments of Shannon Evenness Index (E) of ALOS ordered by overall accuracy (OA %) using the *z*-statistic. Significantly different layer pairs with 95% confidence (z ≥ 1.96) are boldfaced.

		1	2	3	4	5	6	7	8	9	10	11	12	13	14	15	OA%	Ka
1.	IMAGE+ASPECT+DEM+SLOPE+SOLAR RADIATION																80	0.75
2.	IMAGE+ASPECT+DEM+SOLAR RADIATION	0.52															77	0.71
3.	IMAGE+SLOPE+ASPECT+SOLAR RADIATION	0.77	0.25														76	0.70
4.	IMAGE+DEM+SOLAR ADIATION	0.77	0.25	0.00													76	0.70
5.	IMAGE+ASPECT+DEM+SLOPE	1.01	0.49	0.24	0.24												74	0.68
6.	IMAGE+DEM+SLOPE+SOLAR RADIATION	1.49	0.97	0.72	0.72	0.48											71	0.64
7.	IMAGE+ASPECT+SLOPE	1.49	0.97	0.72	0.72	0.48	0.00										71	0.64
8.	IMAGE+SOLAR RDIATION+SLOPE	**1.96**	1.44	1.19	1.19	0.94	0.46	0.46									69	0.61
9.	IMAGE+DEM+SLOPE	**1.96**	1.44	1.19	1.19	0.94	0.46	0.46	0.00								69	0.61
10.	IMAGE+ASPECT+DEM	**2.18**	1.66	1.41	1.41	1.17	0.69	0.69	0.23	0.23							67	0.59
11.	IMAGE+SOLAR RADIATION	**2.18**	1.66	1.41	1.41	1.17	0.69	0.69	0.23	0.23	0.00						67	0.59
12.	IMAGE+ASPECT+SOLAR RADIATION	**2.87**	**2.35**	**2.10**	**2.10**	1.84	1.37	1.37	0.90	0.90	0.67	0.67					63	0.54
13.	IMAGE+SLOPE	**2.87**	**2.35**	**2.10**	**2.10**	1.84	1.37	1.37	0.90	0.90	0.67	0.67	0.00				63	0.54
14.	IMAGE+ASPECT	**3.09**	**2.56**	**2.31**	**2.31**	**2.06**	1.58	1.58	1.12	1.12	0.89	0.89	0.22	0.22			61	0.52
15.	IMAGE+DEM	**4.23**	**3.68**	**3.43**	**3.43**	**3.17**	**2.68**	**2.68**	**2.21**	**2.21**	**1.97**	**1.97**	1.30	1.30	1.08		54	0.43
16.	IMAGE	**5.69**	**5.11**	**4.85**	**4.85**	**4.57**	**4.06**	**4.06**	**3.57**	**3.56**	**3.32**	**3.32**	**2.62**	**2.62**	**2.39**	1.29	46	0.32

3.2.5 Multicollinearity in the input layers in neural network

Same input layers without having multicollinearity problem, as used in woody species diversity mapping such as band 1, 2, 4 and 6 of TM and bands 1, 2 and 4 of ALOS (Appendix 1 and 2) had been used to map woody species evenness also. Mapping accuracies of Shannon evenness index obtained from the confusion matrices resulted in NN with input image layer combinations which do not have multicollinearity problem have been presented in the following Appendix 5, along with respective accuracies (and Kappa statistic) obtained by using all the bands (6 for TM and 4 for ALOS) of both imageries for easy comparison. When we campare overall accuracies of pair combinations without multicollinearity (TM_Multi and ALOS_Multi) against with multicollinearity (TM_All and ALOS_All) of both imageries, we notice that the accuracy without multicollineared layers drop or remains equal with respect to that obtained using all layers with multicollinearity. As for TM, highest accuracy drops from 83% (with multicollinearity) to 81% (without multicollinearity). For ALOS, highest accuracy remains constant (80%) with or without multicollinearity. But the reductions in accuracies are not significant. We realized from the previous similar statistical significance test results with the z values that a layer pair becomes significantly different when the overall accuracy difference between them are at least 10% (e.g. 91% and 81% accuracies are significantly different with z value 2.19, Table 3.3). Taking that advantage, the z values of respective layer pairs of both imageries with and without multicollinearity problem were not calculated but on the light of the previous statement it is observed that for all of the layer pairs the difference in accuracy is less than 10% except combination no 15 for TM (IMAGE+ASPECT); therefore most of them are not significantly different. That is to say, multicollinearity does not significantly reduce the overall accuracy of the produced evenness map.

3.2.6 Effect of image number of bands on mapping accuracy

The overall mapping accuracy of TM is greater than ALOS while using all the bands of both imageries. To investigate whether TM (despite having coarser spatial resolution than ALOS) map woody species evenness more accurately due to possessing more number of bands, we had run the NN with similar first 4 bands of TM (band 1, 2, 3 and 4) that coinciding with 4 bands of ALOS (1, 2 3 and 4). Appendix 6 shows the overall accuracies and respective Kappa statistic of output maps.

Comparison of accuracies of TM map using 4 bands (TM_4) against its all bands (TM_6) indicate that for all of the combinations the accuracy drops (e.g. combinations 4, 5, 16) or remains equal (e.g. combinations 1, 3, 10) in TM_4 than

TM_6 but for all of the combinations, the differences in accuracies are insignificant (e.g. in combination 16, 57% and 59% respectively for TM_4 and TM_6) (Appendix 6). That is using of 4 bands of TM does not significantly reduces the accuracy than using 6 bands.

For TM 4 and ALOS case, accuracies are higher in TM 4 than ALOS for all of the layer combinations; in some combinations significant (e.g. 6, 10, 13 or 16) as the accuracy difference of the layer pairs is 10% or more (although in this case, z-value was not calculated but experience from previous calculations shows that a difference of 10 between two accuracies indicate significant). That is despite removing two bands from TM, accuracy obtained by TM is still higher than ALOS; in some cases significantly higher.

3.2.7 Overlapping forest type map of Majella with diversity map

Table 3.12 shows the result of overlap of forest type map with highest accuracy (83%) TM evenness map. Major evenness class in each forest type has been boldfaced. Good agreement exists between the average value of SEI in each forest type with the majority portion of that forest type belonging to the respective or nearby evenness map classes, except the case of deciduous oak woods. In deciduous oak woods, average value of SEI is 0.61 which belongs to *Low* range of the evenness classes, but the majority proportion of the evenness map falls under *Very High* evenness class. In other forest types very fair agreement exist between; like average value of SEI of beech forest is 0.40 belonging to *Very Low* range of evenness classes while majority area of evenness map (37%) falls under *Very Low* class of evenness as well.

Table 3.12: Result of overlapping TM highest accuracy evenness map with forest types map of Majella along with average values of Shannon Evenness Index (SEI) in each forest types. Major diversity class in each forest type has been boldfaced.

	Evenness Class (%)					
Forest types	Very High	High	Medium	Low	Very Low	SEI* (avg)
Beech	23	31	3	7	**37**	0.40^{VL}
Black/Aleppo Pine	**45**	14	19	16	7	0.67^{M}
Evergreen Oak	17	11	12	12	**48**	0.34^{VL}
Hop-hornbeam	**38**	21	16	16	9	0.82^{H}
Deciduous Oak	**38**	5	25	15	18	0.61^{L}

SEI*= average value of Shannon Evenness Index in each forest types; Diversity Classes, L=Low; VL=very Low; M= Medium; H= High; VH= Very High

Chapter 4: Discussion

It is a long-standing interest of Biogeographers to measure patterns of species occurrence and diversity from space (Gillespie et al., 2008). Incorporation of satellite data with climate, topography data improves the model significantly (Gillespie et al., 2008). In this study we demonstrate how satellite data can be effectively used to map woody species diversity and evenness. We also demonstrate how ancillary environmental data improve the accuracy of woody species diversity and evenness maps significantly when jointly used with satellite data.

4.1 High map accuracy

Two satellite imageries, TM and ALOS were compared to be used for mapping woody species diversity and evenness. Both of the imageries produced species diversity and evenness maps with high accuracy due possibly to comparatively homogeneous canopy structure of this forest site with forest types dominated by several trees (24 all together). We claim for high accuracy as the overall accuracies of the diversity maps obtained using TM and ALOS are 91% (Kappa 0.89) and 81% (Kappa 0.77) respectively; while for evenness maps overall accuracies are 83% (Kappa 0.79) and 80% (Kappa 0.75) respectively for TM and ALOS; both are quite high when compared with the similar published works by other researchers applying different methods. Cayuela, et al., (2006) modelled plant diversity in tropical montane landscape using climatic, biophysical and landcover data with ETM+ NDVI with Generalized Linear Model (GLM) which explained 44% of the overall variability of tree diversity. Foody and Cutler (2003) used NN and standard deviation of nearest pixels and achieved a Pearson correlation coefficient of up to 0.52 between remotely sensed estimate and field data on plant diversity. In a later work, Foody and Cutler (2006) with the attempt to map biodiversity indices of species richness and evenness found satellite data (TM) explaining 69% of the variation in field species diversity. This is the only study we find which engulfs both species evenness and diversity. Rocchini, (2007) estimated ecosystem α-diversity by correlating spectral heterogeneity with environmental spatial heterogeneity and found, Quickbird, ASTER, Landsat ETM+ and re-sampled 60m ETM+ image spectral heterogeneity showing correlation coefficient (r) 0.69, 0.43, 0.67 and 0.69 respectively with ecosystem species diversity. Gould (2000) mapped species diversity in the Hood River area in Canadian Arctic, using NDVI variability of TM data, which explained 65% to 79% variation using only NDVI and NDVI with landcover data respectively. Sobhan (2007) mapped woody species richness in Majella in Italy using hyperspectral airborne data with 0.83 goodness of fit

(r^2=0.83). Nagendra and Gadgil (1999a) made supervised classification of Indian Remote Sensing Satellite (IRS) 1B LISS 2 imagery and obtained 7 broad landcover classes (though the article title mentions it as species diversity) with 88.8% and 89.4% accuracy using 68 random points and 246 quadrates data respectively. In another study, Nagendra and Gadgil (1999b) using the same IRS 1B LISS 2 data, classified 12 landscape ecotypes at Western Ghats-West coast in India with accuracy levels ranging from 70.3% to 91.7%. Based on the above mentioned published works, we can say that the present work advocates itself to be premier of its kind on the topic with highest level of accuracy in diversity mapping. (Worth mention here, studies which involve landscape level classification of species diversity have been included in the discussion while other studies which involve identification and mapping of single species or few species or land cover classification which does not necessarily dictate species diversity or richness mapping have been excluded, as they are different from present study approach and theme). As there is no study we find regarding mapping woody species evenness except Foody and Cutler (2006), we can unequivocally justify this work as a significant contribution in remote sensing woody species evenness.

Overlapping the diversity and evenness maps with forest type map of Majella is an extra check for the accuracy of produced diversity and evenness maps. We noticed in the field, beech forest sustains the majority of the composition as Beech (*Fagus sylvatica*) along with few other species like Pubescent Oak (*Quercus pubescens*) and Linden/Lime (*Tilia cordata*) especially in the lower altitude (800/900-1000/1200m). Therefore majority area of beech forest (34%) belonging to the *Medium* diversity class (with average SDI value 0.65) is reasonable (Table 3.6). Further, as beech forest is mostly dominated by Beech (*Fagus sylvatica*), species evenness is *Very Low* (average SEI 0.40) with 37% of the evenness map falling under *Very Low* class (Table 3.12). black/aleppo pine stands are mainly plantations with the species Black Pine (*Pinus nigra*) and Aleppo Pine (*Pinus alepensis*) along with some other conifers and broadleaved species. Canopy structure of the conifers is alike; therefore image spectral variation is less. Majority portion of the diversity map of this forest (34%) belongs to *Low* diversity class (average SDI 0.34). As the conifers like black/aleppo pine has small and extensively porous crown, other versatile woody species are associated in this forest due to sufficient available sunshine; also ground level vegetation contributes to the recorded reflectance. Therefore, species evenness of this forest is *Very High* with majority area (45%) belonging to the *Very High* evenness class. Evergreen Oak wood is composed mainly of Evergreen Oak (*Quercus* spp) with very few other species like Pubescent Oak (*Quercus pubescens*); therefore in this forest, maximum areas fall to the *Low* diversity (39%) and *Very Low* evenness (48%) classes. hop-hornbeam forest and deciduous oak woods are comparatively more heterogeneous with mix up of several other woody species like Mona Ash (*Fraxinus ornus*), different Mapple (*Acer* spp), Norway Spruce (*Picea abies*), Tilia/Linden (*Tilia cordata*), Common Labrum (*Laburnum anagyroides*) and shrubs. Therefore, majority areas of hop-hornbeam forest (39%) and deciduous oak forest (34%) belongs to higher diversity areas. Also majority areas (38% for both) of these two forest types belong to *Very High* evenness class. Hence, classified TM diversity and evenness maps are in very good agreement with each other as well as with the widely used forest type map of Majella, which was prepared by park experts in the field. Of course, one thing needs mention here is that forest types are very broad vegetation category named by dominant species of each and the accuracy of the forest type map is not reported (by park authority); therefore can not be relied for high precision.

Besides, spatial autocorrelation check was done by ArcGIS 9.3 to ascertain the existence of autocorrelation in the field data sets. We did not find any autocorrelation in the data for the Shannon Diversity Index (H) for all of the 100 sample plots (Moran's I= 0.06 and Z score of the data standard deviation = 0.77). Of course, for Shannon Evenenss Index (E), sample points showed a little bit clustering behaviour (Moran's I= 0.12 and Z score of the data standard deviation = 1.43) which is acceptable. Therefore, the provided information further testifies that the map accuracy obtained is beyond dispute.

Very high resolution imageries like Quickbird definitively facilitate direct identification of species and mapping distribution and diversity, but they incur very high cost which might be beyond reach of many researchers and nature managers especially in the developing countries. High accuracy obtained by easily obtainable imageries like TM and ALOS is without doubt a big advancement in remote sensing tree diversity.

4.2 ALOS maps less accurately than TM

For training ALOS, 10m transect and for TM, 30m transect data were used. Question might arise, is 10m plot/transect size enough to capture the woody species diversity information of an area? We would attempt to link the spectral variation hypothesis (SVH) (Palmer et al., 2002) here to find the answer of this question. SVH states that, higher the spatial variation within the environment, higher the spectral variation (variation in remotely sensed spectral response) which in turn relates to greater ecosystem heterogeneity or species richness/diversity. Simply spoken, areas with higher spectral variation in the remotely sensed data (which can be estimated from the imagery by using standard remote sensing software) will support higher species diversity.

Rocchini et al., (2004) using SVH at varying spatial scale to estimate species richness observed that variation in plant diversity is related to the spectral properties of the environment and scale dependent. And of course, it is established that ecological processes functions at different scale (Dungan et al., 2002). Palmer et al., (2002) correlated spectral heterogeneity with species richness and hypothesized that spectral variation will better predict species richness at micro-scale than at macro-scale. He also supposed that spectral heterogeneity holds promise for species richness mapping and "The weakness of the correlation may be due, in part, to inaccuracies in geo-referencing, differences between the time of image and that the sampling, and inherent variation in species richness of small plots". On the contrary, Rocchini et al., (2004) in a later development explicated that spectral variation is less captured at macro-scale than at micro-scale. He found the spectral heterogeneity explains 20% variation of species richness at micro-scale ($100m^2$) and nearly 50% at macro-scale ($10000m^2$ or 1 ha.). Therefore, we argue from these facts that variation in remotely sensed spectral response or in turn environmental variation or ultimately variation in species diversity are better captured at 30m scale than at 10m scale. Hence, TM produces woody species diversity map more accurately than ALOS.

However when direct approach of species diversity and evenness mapping is involved, spectral heterogeneity proposition might not hold true, because this approach identifies the individual trees and map their distribution directly from imagery. Combined distribution map of all the under consideration species gives the species diversity/richness map (e.g. Sobhan, 2007; Carleer and Wolff, 2004). But indirect approaches such as this study, where the focus is mainly on mapping woody species diversity as the assemblage or overall pattern of diversity by using surrogate measure (e.g. diversity index), and spectral heterogeneity proposition absolutely holds fit. Besides, woody species generally possess wider canopy; thus very few trees may occupy the whole space of a 10m plot. In the worst case, if the canopy of species are extensive in nature, even one single individual may occupy lion's share of the 10m plot space; consequently species diversity of that plot would be very low or zero (0). (Average canopy diameter of some medium aged species in Majella like Beech, Pubescent Oak, Black Pine, Hop-hornbeam, Linden and Ash are roughly 6.5, 7, 4, 6, 5.3 and 5.8 meters respectively). On the other hand, a 30m plot is enough to capture at least several big woody species, indicating higher diversity index. In addition, although a total of 24 woody species were found in all the 100 surveyed sample plots, woody species average canopy in Majella is structurally simple, homogeneous with monotonous continuation of similar canopy over extensive areas. Therefore, definitively, it would be difficult to detect variation in canopy structure (spectral heterogeneity) by satellite data at very smaller scale (like 10m plot). As we know, each of the objects has its own reflectance properties, individual woody species with their own reflectance capacity must have significant contribution on above canopy reflectance recorded by space-born sensors to detect the variability among them. Wider canopy unit (as such 30m plot) elements (species) have greater chance to contribute individually on the above-canopy reflectance variability. These explain partially why lower spatial resolution TM imagery captured woody species diversity and evenness more accurately than higher resolution ALOS imagery.

Another cause of less accuracy for ALOS than TM might be due to the selective availability error (SA error) of the iPAQ GPS used in the study affecting ALOS more than TM. SA error of normal GPS is the deviation of coordinate positions from their true position. This problem could possibly be eliminated by using differentially corrected GPS (DGPS) but this study could not avail the DGPS facility due to limited logistic and financial support (but we find numerous examples of vegetation studies using handheld GPS in recognized peer reviewed journal articles even in Majella e.g. van Gils et al., 2010; Cho and Skidmore, 2009; van Gils et al., 2008; Cho et al., 2007; Boteva et al., 2004). Maximum SA error for normal GPS is 10m, although our experience in the field indicated 1 to 5m (also experienced by Dr. Hein van Gils, an ITC faculty working in Majella for several years) depending on the surroundings. In the deep forest, off course, the SA error varied in its normal range (up to 10m). Consequently the effect of SA error was more in ALOS than TM due to their differential spatial resolution and training data plot size. Maximum deviation due to GPS SA error (10m) incurs displacement of field plot centre 10m away from the true centre in any directions, indicating remotely sensed information totally different from diversity information of original 10m plot size, though sudden change of vegetation composition is not noticed in such close proximity in nature. For TM imagery that is to say 30m plot size, deviation of true plot location in satellite data will not affect significantly. Our field experience and result strongly support the idea that 10m plot size was really not a feasible spatial unit to link woody species diversity with satellite data.

Overall accuracies of diversity maps of both imageries are quite high, if not 100%, in comparison to others work on the issue. Accuracy more than what is achieved could not be materialized due mainly what we anticipate to errors in geo-referencing imageries, deviation of the plot coordinate positions due to selective availability error of the handheld GPS machine, inherent variation in species diversity in the plots and difference in field plot diversity information with the remotely sensed information due to overcast of some dwarf tree canopies by dominant tree canopies. From the field experience it was noticed that in many of the surveyed plots, several individual trees were dwarf with their canopies overcast by wider canopies of dominant trees. Although they were tree species, they did not have contribution in the over-canopy reflectance, hence not recognized by the sensors.

Image spectral resolution (number of bands) is a crucial factor to compensate for its lower spatial resolution in the study of species diversity (Rocchini, 2007). He (Rocchini, 2007) found, Quickbird and re-sampled 60m Landsat ETM+ imageries' spectral heterogeinity when correlated with species richness, both came up with same correlation coefficient of 0.69 (r=0.69); where Quickbird has 2.88m spatial resolution with 4 multispectral bands while re-sampled 60m ETM+ has 6 bands. On the contrary, in the same study, ASTER imagery showed less correlation coefficient (r=0.43) despite possessing higher spatial (15m and 30m) and spectral resolution (9 bands used). Therefore, higher spatial resolution or pixel size is not the only determining factor, as widely celebrated concept, for high accuracy mapping of species diversity. In fact, image spectral variability is scene and sensor dependent (Rocchini et al., 2007; Mehner et al., 2004; Woodcock and Strahler, 1987). Nagendra (2001) dealing with image classification for vegetation diversity study noted that, if the spatial resolution is too high than the object to represent, variability may increase and image classification accuracy decrease. Besides, the widely believed concept that higher spatial resolution generates higher mapping accuracy is not true for all environments and mapping scales (Rocchini, 2007). It is not absurd to mention here that even hyperspectral HyMap data (126 bands, 4m) could not estimate grassland biomass with high accuracy (>50%) in the same national park Majella (Cho and Skidmore, 2009). These known facts are congruent with the finding of the present study. ALOS imagery posse 10m spatial resolution with 4 spectral bands while TM has 6 bands (used) with 30m spatial resolution. Ecosystem spatial heterogeneity and in turn species diversity and evenness were better recorded (as image spectral heterogeneity) by TM than ALOS due to the inherent characteristic of the sensor and possessing higher spectral resolution (and as diversity is scale dependent- Rocchini et al., 2007) TM showed superiority over ALOS on mapping accuracy of woody species diversity and evenness (as spectral variation is scene and sensor dependent) in the present context of vegetation structure (scene) in Majella.

Further, the overall accuracies drops while 4 bands of TM are used (TM_4) than 6 bands (TM_6), though the difference is insignificant for most of the combinations in both diversity and evenness maps, and significant for very few combinations for diversity map. The overall accuracies obtained using 4 bands of TM (TM_4) are still higher than those obtained using all bands of ALOS in most of the combinations for both diversity and evenness, though the differences are insignificant for diversity and significant in some combinations for evenness. These findings testify that number of bands (spectral resolution) of imageries is a contributing factor in the mapping accuracy of diversity and evenness of woody species. These evidences also testify that inherent characteristic of TM to catch diversity and evenness is better than ALOS, besides number of bands; as the accuracies are still higher using 4 bands of TM (TM_4) than ALOS.

4.3 Environmental layers increase accuracy

Imageries alone could not produce high accuracy map due possibly to similar spectral response from different species (e.g. Yang et al., 2007) as different plants respond to electromagnetic spectrum differently (Verbyla, 1995); also as homogeneous canopy structure exist in Majella. All species can not be separated easily by remote sensing (Price, 1994). However, it is not surprising that ancillary environmental data increases the map accuracy tremendously. In fact, effect of various topographic or climatic factors on vegetation e.g relief, elevation, terrain shape, energy, evapotranspiration, latitude etc are well documented over centuries, as mentioned earlier. Further, altitudinal gradation of vegetation composition and distribution is conspicuous in Majella (as detailed in study site description). Environmental data layers like elevation, slope, aspect and solar radiation that we used in this study affect woody species diversity directly or indirectly, the result of which is obvious in the obtained map accuracy. However, present study findings indisputably tally with some of the published texts on similar matter. O'Brien et al., (2000) studied the climatic gradients in woody plant diversity and noted that when relief is added as a third variable in the model, explanatory power (R^2) increases to 7-12%. Gould (2000) mapped species richness in the Hood River area in Canadian Arctic, using NDVI variability of TM data, which explained 65% variation in species richness by correlation while only imagery was used and 79% variation while NDVI was jointly used with vegetation map of the area. Schmidt et al., (2004) reported overall map accuracy promotes from 40% to 66% (26% increase) when topographic layers (elevation, slope, aspect and terrain position) were included with image in coastal saltmarsh vegetation mapping in the Netherlands. Yang et al., (2007) found mapping accuracy increases 14% and 15% in two different classifiers to map forest types at Yunnan province in China. Janssen et al., (1990) documented 12% and 20% increase in accuracy of land-cover classification by remote sensing data in two different agricultural regions in the Netherlands. Franklin et al., (1994) reported that classification accuracy had increased from 62% while used only TM image to 73% while DEM was incorporated to map alpine vegetation in Canada; and identification of species increased from 81 to 91%. In another study Franklin (1994) indicated when DEM was incorporated, forest classification accuracy increased from 96 to 97% while species identification accuracy increased from 91 to 100%. In fact, effect of topographic and climatic factors on vegetation is well known but less used in mapping their diversity and evenness.

4.4 Multicollinearity

Some bands were excluded in the NN for both diversity and evenness to avoid problems of multicollinearity among some of the bands of TM and ALOS and to see how it affects the accuracy. This practice, however, is not a new phenomenon and exercised in several publications referring to the application of satellite data for various purposes e.g. forest biomass assessment (Jong et al., 2003), forest inventory (Salvador and Pons, 1998), crown cover estimation (Xu et al., 2003), vegetation mapping (Brook and Kenkel, 2002), forest diversity mapping (Cayuela et al., 2006) etc. Our findings indicate that when multicollineared bands of TM (band 3 and 5) and ALOS (band 3) are not used in the NN, the accuracy of diversity map is not affected significantly for both the imageries and in case of both diversity and evenness. For TM, removing multicollineared bands reduced the accuracy significantly for only 2 pair combinations (Table 3.3) in diversity mapping; for all other cases, accuracy reductions were not significant for both cases of both imageries. The cause of the phenomenon is due to the fact that all bands of the imageries are not equally important for species diversity mapping. It is well established that some bands are good for estimating biomass and growth (e.g. Boyd et al., 2002; Wang et al., 2005; Lasaponara, 2006). Recently Rocchini et al., (2007) compared the correlation of 4 bands of Quickbird multispectral imagery with spectral heterogeneity for species richness estimation and found that the near infra-red band (band width 0.76-0.90μm) explains 41% variation in species richness, the highest among all other 3 bands (24%, 28% and 25% respectively for bands red, green and blue). They concluded that the potential of Quickbird imagery for species richness estimation is for the near infra-red band rather than three other redundant visible bands. Our study finding, as why removal of multicollineared bands does not significantly reduce the accuracy, tally fully with these findings. Band width of near infra-red band of Quickbird (band no 4, width 0.76-0.90μm) exactly coincides with Band no 4 of TM (0.76-0.90μm) and ALOS (0.76-0.90μm), which is the main contributor of estimating species diversity. Near infra-red (Verbyla, 1995), middle infra-red (Everitt et al., 1987) bands are strongly recommended for species discrimination. This band did not show multicollinearity problem for both imageries and thus was included in all the input layer combinations in NN. That's why big difference in accuracy was not obtained for majority of the combinations with and without multicollinearity. Therefore, our assessment is that while remote sensing woody species diversity and evenness is involved, as by this approach, one should not concern about the multicollinearity problem in image bands (as far as image principal band for catching vegetation diversity is not excluded, as in this case band 4), as presence of multicollinearity does not significantly affect accuracy.

4.5 Field sampling

The method we applied to train 30m spatial resolution TM data by 30m plot size diversity information and 10m spatial resolution ALOS data by 10m plot diversity information, both plots having the same centre, does not require the imageries to be re-sampled to a common spatial resolution to evaluate their mapping accuracy. We did not find sound literature on whether re-sampling reduces the image quality although both up-re-sampling (Yamamoto et al., 2009; Edenius et al., 2003) and down-re-sampling (e.g. Rocchini, 2007; Sobhan, 2007) has been performed in similar studies. But it is anticipated that by downscaling, image's inherent capacity is deteriorated. We kept the spatial resolution of the imageries intact during training in the NN as their original; therefore variation in mapping accuracy by them is due to their inherent capacity to catch species diversity and evenness.

A riddle needs highlight at this point, as associated with values of diversity and evenness indices due to unequal field plot sizes. Differential size of the field sample plots used in this study to train individual imageries might have implications too, to an extent, in the variation of respective Shannon diversity and evenness values. As an example, Shannon diversity index (SDI) for 30m plot size is 0.71 and for 10m plot is 0.97 in field plot no 1. In field plot no 2, SDI is 0.76 at 30m plot size while for 10m plot the value is 0.51. The second fact is reasonable as diversity should be higher at bigger area units and lower at smaller area units. But for the first case, the matter is a little bit crafty. Here, SDI value is greater at low plot area and lower at bigger plot area. Of course, this trend is not true for majority of the sample plots. In reality, count of the species at each size of plot (and so respective Shannon diversity and evenness values) varies with the orientation of the line transects with respect to the spatial distribution and arrangement of available species in field plots. And so, the Shannon diversity and evenness indices values will vary with respect to the layout of the two transect lines in each plot. Thus, different transect layouts will produce different diversity and evenness indices values due to variation in species composition along each alternative layouts in the same plot. That is to say, different transect layout will have different indices values in the same plot. Furthermore, in nature, arrangement and spatial pattern of occurrence of species varies at different spatial scales, say from the plot centre. In some cases, species show gregariousness in occurrence while in other cases sparsely distributed in the plots. Even both situation, i.e. gregariousness and sparseness can coexist in the same plot but at different spatial scales with even barren space in-between. Therefore, if species assemblage exists near the plot centre, then at smaller spatial scale (i.e. 10m), calculated species diversity values may be higher than that from bigger spatial scale (i.e. 30m), as the smaller scale area can accommodate major portion of the species assemblage; thus high diversity and evenness values. For many of the sample plots, we experienced this situation in the field. Of course, when similar pattern of gregariousness occurs uniformly throughout the largest spatial extent under consideration (i.e. in our case 30m), opposite fact will hold true i.e. bigger plot size definitely will have higher index values which is normal.

When uniform spatial plot size ground data is used for training differential spatial resolution imageries, imageries must be re-sampled to a common pixel size corresponding to ground sample plot (as we see in some studies); and thus intra-plot variation in measuring values of indices of diversity and evenness are not concerned, but re-sampling (we don't say categorically as no supporting literature exist) reduces the inherent capacity of higher resolution imageries. To train various spatial resolution TM and ALOS imageries with field data by keeping the spatial resolution as they are, we found this sampling strategy as the best alternative despite having controversy in the diversity and evenness indices values at same as well different spatial scales within the field plot as indicated above. Worth taking note here that the variation in woody species diversity and evenness information within the plot at different spatial scale will not affect the accuracy of classified imageries as each pixel represent the spatial ground unit as a whole and irrespective of transect layout for ground field data. Furthermore, if we consider the data sets of 10m and 30m plot sizes having same plot centre as independent (and it is so in this study), they will be classified as different diversity and evenness classes according to recorded respective species composition as a whole irrespective of layout of transects inside. To say more explicitly, as in previous example of plot number 1, SDI value of 30m plot is 0.71 which falls under *Medium* diversity class (SDI value range 0.64-0.94); on the other hand SDI value of 10m plot is 0.97 which falls under *High* diversity class (SDI value range 0.96-1.14), although both of the plots are eccentric. Therefore, same cantered ground data or pixels may be classified under different diversity levels (also evenness) independently with respect to the spatial unit (pixels) of imageries. Hence intra-plot variation of indices values (as discussed) will not affect the map accuracy. This, in turn, relates to our discussion of fact (done earlier) that species diversity is scale dependent; also variation in remote sensing capacity of species diversity is dependent on inherent capacity of the imageries and their spatial and spectral resolution. But care should be taken during setting layout of the transect lines in each plot so that they can reflect real species composition of the plot without over or under estimating species information of that plot; and similar trend should be maintained for all spatial scales of that plot (i.e. 10m or 30m).

This study could not avail ALOS and TM imageries acquired at the same data (synchronized) or with very narrow lag of acquisition dates as ALOS data is not free to obtain and not available before 2006 (launched on Jan 24 ‘06) while TM data not available after 2003. Two imageries of ALOS acquired on 15 July’07 and 20 July ’09 were available at ITC for students use. Therefore, to minimize year gap between acquisition dates of two imageries, we used ALOS of 15 July’07 with TM of 27 Sep’03. However, we find instances of vegetation studies with such year gap of image acquisition in the existing literature. Moreover, 4-years are not a significant time for occurring significant change in nature, especially in woody species composition and structure of a geographical area unless catastrophic events happen. Therefore, we do not expect significant variation in map accuracy due to non-synchronized ALOS and TM acquisition date.

4.6 Ecological implications

Current study typically focuses on mapping woody species diversity and evenness of a central Italian forest area as the principal endeavour. However, some ecological facts were revealed as the by-output of the whole research process. Study site in Majella is a mountainous landscape with mount Morrone (second highest peak) passing through the centre of it. Altitude is a principal regulatory factor governing the distribution and diversity of vegetation in the region (which is also documented by other studies e.g. Stanisci et al., 2005). Change in diversity is less prominent at lower altitude than at higher altitude. Vertical gradation of vegetation with altitude is very evident, and noticed in the spatial extension and arrangement of typical forest types as a broad pattern; so as the species diversity and evenness. As example, beech forest was found confined to the specific phytoclimatic belt Montane (900/1000-1600/1700 m) with average SDI 0.65, belonging to *Medium* diversity class. Deciduous oak woods are mainly found below 900m altitude in the sub-Mediterranean belt with average SDI 0.72, belonging to *High* diversity class. Diversity and evenness classes vary widely with the forest types due mainly to other associated species in each type beyond the dominant one, along with altitude. As for example, highest average SDI (1.14) and SEI (0.82) were found in the hop-hornbeam forest situated at wide altitudinal range (500-1200m) while lowest average SDI (0.52) and SEI (0.34) were found in the evergreen oak woods situated in the lower altitude (up to 500m). Of course that does not necessarily mean that woody species diversity is high at the higher altitude and low at the lower altitude. Rather the opposite trend (decreases of species diversity with altitude) is true. Indeed, generally say, the Mediterranean (<500m) and sub-Mediterranean (500-900m) phytoclimatic belts are the most species rich and even with different species while Montane belt (900-1600m) is the least with solely dominated by Beech (*Fagus sylvatica*). The forest types are basically broad categorization of the woody vegetation of the park, each of them occupying broad altitudinal ranges, and scale of that variation as 'forest stands' is wide too. For example "beech" is short for broad-leaved mesophilic deciduous forest; mostly beech but at lower altitudes (e.g. 800-1000m) mixed with e.g. maples (*Acer* spp), Pubescent Oak (*Quercus pubescens*) and Linden/Lime (*Tilia cordata*). As the altitudinal range of occurrence of some of the forest types overlaps, so variation in average SDI or SEI values of each of them basically does not narrowly attribute to altitude but very broadly. But variation of the diversity and evenness of woody species among the forest types is distinct (Jiang et al., 2007). Of all forest types, hop-hornbeam forest is the most diverse and even while evergreen oak woods are the least diverse and even.

We revealed good agreement between the produced diversity and evenness maps while they are overlapped with the forest type map of Majella. Broadly, areas with high woody species diversity overlap with areas of high species evenness. Mentionable as example, majority portion of hop-hornbeam forest belongs to high diversity (32%) and evenness (38%) class with highest average value of SDI (1.14) and SEI (0.82). This phenomenon is, of course, very much usual. Plots or areas with more number of species will definitely count for higher diversity and evenness as diversity and evenness go concurrent to each other.

Level of influence of independent climatic and topographic factors (site factors) regulating plants' life, diversity and distribution varies from each other. Some elements are more important than others. Therefore, environmental layers used in the study, which can also be termed as site factors regulating vegetations' life have dissimilar affect on diversity and evenness of woody species, finally on produced map accuracy. Slope proved to be the most influential factor affecting map accuracy of woody species diversity for both TM and ALOS imageries while for evenness, solar radiation was the most important regulatory factor for both imageries.

The level of diversity and evenness we get in Majella is not high in comparison to some other studies. Jiang et al., (2007) reported average Shannon-Weiner index value as 2.03 in deciduous broadleaved forest and 1.90 in temperate evergreen coniferous and deciduous broadleaved mixed forest in northwestern China. Jing et al., (2004) documented SDI ranging from 0.92-1.96 and SEI from 0.15-0.46 at different altitude belts (1100-1700m) in a coniferous forest at Changbai mountainous landscape in northeast China. Marsden and Pilgrim (2003) studied tree diversity of two lowland rainforest sites on New Britain in Papua New Guinea and reported SDI value at different habitats ranging from 1.63 to 2.38. Therefore, we can say that woody species diversity in Morrone is comparatively neither high nor low, rather of an intermediate level.

Chapter 5: Conclusion and recommendation

5.1 Conclusion

The study demonstrate that remote sensing and environmental data can be effectively used to derive accurate information regarding woody species diversity and evenness (two integral components of biodiversity) of an Italian, relatively homogeneous (up to 24 species) forest site. At this point answers of the research questions need evaluation.

Question 1: Can TM and ALOS imageries be used for mapping woody species diversity and evenness?

We mapped the woody species diversity and evenness of Majella by TM and ALOS imageries with high accuracy. Accuracy level obtained is beyond dispute as training and accuracy assessment were done by independent data sets which are not spatially auto-correlated. Accuracy assessment was done by standard and widely used method by generating error matrix.

Question 2: Which image produces more accurate woody species diversity and evenness maps, TM or ALOS?

TM produces woody species diversity and evenness maps with higher accuracy than ALOS imagery. Comparison of the overall accuracies and respective Kappa statistic of produced diversity and evenness maps shows TM outputs are more accurate than ALOS.

Question 3: Does the ancillary environmental data (elevation, slope, aspect, solar radiation) significantly improve the mapping accuracy of woody species diversity by satellite data?

Our results suggest that relatively simple incorporation of ancillary environmental data very significantly increases the accuracy of both species diversity and evenness maps. In some cases the accuracy was multiplied itself to double when all the input layers were jointly used in NN classifier.

Question 4: How the woody species diversity and evenness do vary with forest types and altitude gradients?

Variation of diversity and evenness is prominent with forest types and altitude. At higher altitude, overall pattern of woody species diversity and evenness is less than at lower altitude.

Findings of this study includes: i) Both TM and ALOS imageries can be used for mapping woody species diversity and evenness with high accuracy ii) Imagery with higher spatial but lower spectral resolution does not produce higher accuracy species diversity map; rather coarser spatial resolution imagery with higher spectral resolution produces woody species diversity and evenness maps with higher accuracy iii) Use of ancillary environmental data along with satellite data tremendously increases the mapping accuracy of woody species diversity and evenness iv) Presence of multicollinearity among some of the bands of both imageries does not significantly reduce or enhance the mapping accuracy of both richness and evenness, but above all reduces the accuracy at least to an extent v) More number of bands (higher spectral resolution) of TM is a contributing factor to achieve higher mapping accuracy than ALOS vi) Woody species diversity and evenness in Majella vary with forest types and altitude.

Woody species diversity and evenness map can have significant implications in conservation planning and protection of wilderness especially in the areas where there exist huge pressure of rapid road expansion, resource extraction, urbanization, and deforestation. Rapid assessment and monitoring of plant diversity at larger geographical scale is 'critical' for conservation planning but we lack methods (Bawa et al., 2002). Field surveys for large scale estimate of vegetation diversity are unsuitable, uneconomical, inconsistent, frequently unrepeatable and not feasible methods. When wider scale e.g. regional, national or global estimation of plant diversity is concerned, remote sensing might proof economical, easily obtainable, regularly repeatable and superior than any other methods. Remotely sensed data are biologically relevant, spatially extensive, calibrated and therefore temporarily consistent.

The approach presented in this paper maps woody species diversity and evenness pattern with high accuracy that would be replicable at larger scale. No study has included both species diversity and evenness together, and combined environmental data with the satellite data by this approach, as we did; thus promoting the study as a premier on the issue. The approach presented in this paper is to supplement rather than replace the existing methods of mapping species diversity. But we confidently believe that this approach exerts superiority over other existing approaches of mapping pattern of woody species diversity due not only to highest accuracy obtained till date but also its easiness to implement and operationalize over wider geographical areas.

5.2 Recommendations

Woody species diversity information from 100 field samples was used in this study for training and validation while the area coverage is not so extensive (170 km^2). Replication of the approach for wider geographical areas wood necessitates large number of field sample plot survey, which is quite difficult, time consuming and unrealistic. Further study can be carried out to cover larger areas with reasonably less number of field sample data to investigation how the accuracy fluctuates against present findings. Of course, too less number of samples in relation to the study area may prove ineffective as O'dae et al., (2006) observed significant difference in accuracy to estimate species richness (bird) from limited sample; and Clémentine (1998) concluded, whatever is the sampling strategy, estimation of species richness depends on sample size.

Imageries like ASTER are freely obtainable, has fairly high spatial resolution (15 to 30m) and spectral resolution (15 bands), which might prove better than both ALOS and TM in estimating woody species diversity. Present approach may be applied to ASTER imagery. Although Rocchini (2007) reported ASTER is less efficient in linking spectral heterogeinity to species diversity/richness (r= 0.43), it is yet to be tested by NN approach presented in this paper. We expect much better accuracy by ASTER in NN due to its higher spectral resolution.

Other versatile ancillary environmental data like topographic (e.g terrain position), climatic (temperature, precipitation, potential evapotranspiration) and other (e.g. landcover) related to plant growth and distribution can also be incorporated in the NN as input layers to examine their contribution in mapping accuracy. It can be recalled that this study used only four ancillary environmental layers (elevation, slope, aspect and solar radiation).

The study could not avail differentially corrected GPS system (DGPS) for recording plot coordinates due to limited per capita instrumental support available at ITC. But we feel that it might be an important factor affecting map accuracy and further study (if launched) should avail DGPS in the field campaign.

References:

Adams, J. B., Smith, M. O. and Gillespie, A. R. 1993. Imaging spectroscopy: Interpretation based on spectral mixture analysis. In C. M. Pieters and P. A. J. Englert (Ed.), *Remote geochemical analysis: Elemental and mineralogical composition,* Cambridge, England: Press Syndicate of Univ. of Cambridge, 145 – 166pp.

Atkinson, P.M. and Tatnall, A.R.L. 1997. Neural networks in remote sensing. *International Journal of Remote Sensing*, 18: 699–709.

Augusteijn, M. F. and Warrender, C. E. 1998. Wetland classification using optical and radar and neural network classification. *International Journal of Remote Sensing,* 19 (8): 1545-1560.

Bawa, K., Rose, J., Ganeshaiah, K. N., Barve, N., Kiran, M. C. and Umashaanker. R. 2002. Assessing biodiversity from space: an example from the Western Ghats, India. *Conservation Ecology,* 6(2): Art 7. [online] URL: http://www.consecol.org/vol6/iss2/art7

Bhattarai, K.R. and Vetaas, O.R. 2003. Variation in plant species richness of different life forms along a subtropical elevation gradient in the Himalayas, east Nepal. *Global Ecology and Biogeography*, 12:327-340.

Bolstad, P. V., Swank, W. and Vose, J. 1998. Predicting southern Appalachian overstory vegetation with digital terrain data. *Landscape ecology*, 13:271-283.
Boteva, D., Geoffrey Griffiths, G. and Dimopoulos, P. 2004. Evaluation and mapping of the conservation significance of habitats using GIS: an example from Crete, Greece. *Journal for Nature Conservation,* 12: 237—250.
Boyd, D.S., Foody, G.M. and Ripple, W. J. 2002. Evaluation of approaches for forest cover estimation in the Pacific Northwest, USA, using remote sensing. *Appl. Geogr,* 22: 375-392.
Brook, R. K. and Kenkel, N. C. 2002. A multivariate approach to vegetation mapping of Manitoba's Hudson Bay Lowlands. *Int. J. Remote Sensing*, 23 (21): 4761–4776.
Carleer, A. and Wolff, E. 2004. Exploitation of very high resolution satellite data for tree species identification. *Photogrammetric Engineering and Remote Sensing,* 70:135–40.
Carson, H. W., Lass, L. W. and Robert, H. C. 1995. Detection of Yellow Hawkweed (Hieracium pratense) with High Resolution Multispectral Digital Imagery. *Weed Technology*, 9:477-483.
Carter, G.A., Knapp, A.K., Anderson, J.E., Hoch, G.A. and Smith, M.D. 2005. Indicators of plant species richness in AVIRIS spectra of a mesic grassland. *Remote Sensing of Environment,* 98: 304–16.
Cayuela, L., Benayas, J. M. R., Justel, A. and Salas-Rey, J. 2006. Modeling tree species diversity in a highly fragmented tropical montane landscape. *Global Ecology and Biogeography*, 15: 602-613.
Chatterjee, S. and Price, B. 1991. *Regression Analysis by Example*, 2nd edn., Wiley
Cho, M. A. and Skidmore, A. K. 2009. Hyperspectral predictors for monitoring biomass production in Mediterranean mountain grasslands: Majella National Park, Italy. *International Journal of Remote Sensing*, 30 (2): 499–515.
Cho, M.A., Skidmore, A., Corsi, F., van Wieren, S.E., Sobhan, I. 2007. Estimation of green grass/herb biomass from airborne hyperspectral imagery using spectral indices and partial least squares regression. *International Journal of Applied Earth Observations and Geoinformation,* 9:414-424.
Chuvieco, E. 1999. *Remote sensing of large wildfires in the European Mediterranean Basin*, Springer-Verlag, Berlin.
Civco, D.L. 1993. Artificial neural networks for land-cover classification and mapping. *International Journal of Geographic Information Systems*, 7: 173–186.
Clémentine, G. C., Raphaël, P., Jean-Pierre, P. and François, H. 1998. Sampling strategies for the assessment of tree species diversity. *Journal of Vegetation Science*, 9: 161-172.
Cohen, J. 1960. A coefficient of agreement for nominal scales. *Educ. Psychol. Meas*, 20: 37–46.
Cohen, W.B. and Goward, S.N. 2004. Landsat's role in ecological applications of remote sensing. *Bioscience,* 54: 535–45.
Colwell, R.K. and Coddington, J.A. 1994. Estimating terrestrial biodiversity through extrapolation. *Philos. Trans. R. Soc. Lond. B,* 345: 101-118.
Congalton, R.G. 1991. A review of assessing the accuracy of classification of remotely sensed data. *Remote Sensing of Environment,* 37: 35–46.

Congalton, R.G., and K. Green, 1999. *Assessing the Accuracy of Remotely Sensed Data: Principles and Practices*, Mapping Sciences Series, Lewis Publishers, Boca Raton, Florida, 137 p.

Congalton, R.G., Oderwald, R.G. and Mead, R.A. 1983. Assessing landsat classification accuracy using discrete multivariate analysis statistical techniques. *Photogramm. Eng. Rem. Sens.,* 49 (12): 1671–1678.

Conti, F. 1998. *Flora D'Abruzzo: An annotated check-list of the flora of the Abruzzo*. Palermo, Herbarium Mediterraneum Panormitanum.

Currie, D. J. 1991. Energy and large-scale patterns of animal and plant species richness. *American Naturalist,* 137 (1):2-24.

Currie, D. J. and Paquin, V. 1987. Large scale biogeographical pattern of species richness of trees. *Nature*, 329: 326-331.

Dahdouh-Guebas, F., van Hiel, E., Chan, J.C.W., Jayatissa, L.P. and Koedam, N. 2004. Qualitative distinction of congeneric and introgressive mangrove species in mixed patchy forest assemblages using high spatial resolution remotely sensed imagery (IKONOS). *Systematics and Biodiversity,* 2: 113–19.

Dirk, V den P. and Bart, L. 2004. Attrition Analysis for Financial Services Using Proportional Hazard Models. *European Journal of Operational Research*, 157 (1): 196-217.

Donkor, S. 2008. Mapping and Impact of Avalanche - created Canopy Gaps in the Majella Beech Forest. *MScThesis*, Faculty of Geo-Information Science and Earth Observation (ITC), Enschede, University of Twente, the Netherlands.

Drobner, U., Bibby, J., Smith B. and Wilson, J.B. 1998. The relation between community biomass and evenness: what does community theory predict, and can these predictions be tested? *Oikos*, 82:295-302.

Dungan, J., Perry, J. N., Dale, M. R. T., Legendre, P., Citron-Pousty, S. and Fortin, M. J. 2002. A balanced view of scale in spatial statistical analysis. *Ecography*, 25: 626−640.

Duro, D.C, Coops, N.C., Wulder, M.A. and Han, T. 2007: Development of a large area biodiversity monitoring system driven by remote sensing. *Progress in Physical Geography,* 31:235–60.

Edenius, L., Vencatasawmy,C. P, Sandström, P. and Dahlberg U. 2003. Combining Satellite Imagery and Ancillary Data to Map Snowbed Vegetation Important to Reindeer Rangifer tarandus. *Arctic, Antarctic, and Alpine Research*, 35(2):150-157.

Everitt, J.H., Escobar, D.D., Blasquez, C.H., Hussey, M.A. and Nixon, P.R. 1987. Evaluation of the mid infra-red (1.45 to 2.0 μm) with a black-and-white infrared video camera. *Photogrammetric Engineering and Remote Sensing,* 52:1655-1660.

Everitt, J.H., Yang, C. and Deloach, C.J. Jr. 2006: Remote sensing of giant reed with QuickBird satellite imagery. *Journal of Aquatic Plant Management,* 43:81–85.

Fairbanks, D.H.K. and McGwire, K.C. 2004. Patterns of floristic richness in vegetation communities of California: regional scale analysis with multi-temporal NDVI. *Global Ecol. Biogeogr.,* 13: 221-235.

Foody, G. M. 2002. Status of land cover classification accuracy assessment. *Remote Sensing of Environment,* 80: 185–201.

Foody, G. M. and Cutler, M. E. J. 2006. Mapping the species richness and composition of tropical forests from remotely sensed data with neural networks. *Ecological modelling,* 195: 37–42.

Foody, G.M. and Cutler, M.E.J. 2003. Tree biodiversity in protected and logged Bornean tropical rain forests and its measurement by satellite remote sensing. *Journal of Biogeography,* 30: 1053–66.

Foody, G.M., Atkinson, P.M., Gething, P.W., Ravenhill, N.A. and Kelly, C.K. 2005. Identification of specific tree species in ancient seminatural woodland from digital aerial sensor imagery. *Ecological Applications,* 15:1233–44.

Franklin, S.E. 1994. Discrimination of subalpine forest species and canopy density using digital CASI, SPOT PLA, and Landsat TM data. *Photogrammetric Engineering and Remote Sensing,* 60:1233-1241.

Franklin, S.E., Connery, D.R. and Williams, J.A. 1994. Classification of alpine vegetation using Landsat Thematic Mapper, SPOT, HRV and DEM data. *Canadian Journal of Remote Sensing,* 20:49-60.

Gillespie, A. R., Smith, M. O., Adams, J. B., Willis, S. C., Fischer, A. F. and Sabol, D. E. 1990. Interpretation of residual images: spectral mixture analysis of AVIRIS images, Owens Valley, California. *Proceedings of the Second Airborne Imaging Spectrometer Data Analysis Conference,* Pasadena, CA. Jet Propulsion Laboratory, 243- 270 pp.

Gillespie, T. W., Foody, G. M., Rocchini, D., Giorgi, A. P. and Sassan Saatchi, S. 2008. Measuring and modelling biodiversity from space. *Progress in Physical Geography,* 32(2):203–221.

Gillespie, T.W. 2006. Predicting woody-plant species richness in tropical dry forests: a case study from South Florida, USA. *Ecol. Appl.,* 15: 27-37.

Goodwin, N., Turner, R. and Merton, R. 2005. Classifying *Eucalyptus* forests with high spatial and spectral resolution imagery: an investigation of individual species and vegetation communities. *Australian Journal of Botany,* 53:337–45.

Gould, W. 2000. Remote sensing of vegetation, plant species richness, and regional biodiversity hot spots. *Ecol. Appl.,* 10: 1861-1870.

Griffiths, G.H., Lee, J. and Eversham, B.C. 2000. Landscape pattern and species richness; regional scale analysis from remote sensing. *Int. J. Remote Sens.,* 21: 2685-2704.

Günter, S., Weber, M., Erreis, R., and Aguirre, N. 2007. Influence of distance to forest edges on natural regeneration of abandoned pastures: a case study in the tropical mountain rain forest of Southern Ecuador. *European Journal of Forest Research,* 126: 67-75.

Haara, A. and Haarala, M. 2002. Tree species classification using semi-automatic delineation of trees on aerial images. *Scandinavian Journal of Forest Research,* 17: 556–65.

Hair, J. F. Jr., Anderson, R. E., Tatham, R. L. and Black, W. C. 1995. *Multivariate Data Analysis*, 3rd edn, New York, Macmillan.

Harrison, S, Ross, S. J. and Lawton, J. H 1992. Beta Diversity on Geographic Gradients in Britain. *Journal of* Animal *Ecology*, 61(1):151-158.

Hepner, G. F., Logan, T., Ritter, N. and Bryant, N. 1989. Artificial neural networks classification using a minimal training set: Comparison to conventional supervised classification. *Photogrammetric Engineering and Remote Sensing,* 56 (4): 469-473.

Hurlbert A. H and White, E. P. 2005. Disparity between range map- and survey-based analyses of species richness: patterns, processes and implications. *Ecology Letters*, *8*: 319–327.

Izsák, J., 2007. Parameter dependence of correlation between the Shannon index and members of parametric diversity index family. *Ecological Indicators*, 7:181-194.

Janssen, L.L.F., Jaarsma, M.N. and van der Linden, E.T.M. 1990. Integrating topographic data with remote sensing for land-cover classification. *Photogrammetric Engineering and Remote Sensing,* 56 (11): 1503-1506.

Jensen, J.R. 1996. *Introductory digital image processing*, Prentice Hall, New Jersey.

Jiang, Y., Kang, M., Zhu, Y. and Xu, G. 2007. Plant biodiversity patterns on Helan Mountain, China. *ACTA OECOLOGICA*, 3 2: 1 2 5 – 1 3 3.

Jing Wei, J., Deng, H., Wu, G. and Zhao, J. 2004. Biological diversity in the coniferous forest on the northern slope of Changbai Mountain, northeast China. *Int.J Sustain. Dar. World Ecol,* 11:181-190.

Jong, S.M. de., Pebesma, E. J., and Lacaze, B. 2003. Aboveground biomass assessment of Mediterranean forests using airborne imaging spectrometry: the DAIS Peyne experiment. *International Journal of Remote Sensing,* 24: (7):1505 - 1520.

Kangas, A. and Maltamo, M. 2007. *Forest inventory methodology and applications,* Springer, Berlin.

Kennedy, P. 1992. *A Guide to Econometrics*, Oxford, Blackwell.

Kent, M. and Coker, P. 1992. *Vegetation description and analysis: A practical approach,* John Wiley and Sons, INC, 623p.

Kumar, L., Skidmore, A.K. and Knowles, E. 1997. Modelling topographic variation in solar radiation in a GIS environment. *International Journal of Geographical Information Science,* 11: 475-497.

Lam, T. Y. and Kleinn, C . 2008. Estimation of tree species richness from large area forest inventory data: Evaluation and comparison of jackknife estimators. Forest Ecology and Management, 255: 1002–1010.

Lasaponara, R. 2006. Estimating spectral separability of satellite derived parameters for burned areas mapping in the Calabria region by using SPOT-Vegetation data. *Ecol. Model,* 196: 265-270.

Lauver, C. and Whistler, J. L. 1993. A hierarchical classification of TM imagery to identify natural grassland areas and rare species habitat. *Photogramm. Eng. Remote Sens.,* 59: 627-634.

Levin, N., Shimida, A., Levanoni, O., Tamari, H. and Kark, S. 2007. Predicting mountain plant richness and rarity from space using satellite-derived vegetation indices. *Diversity and Distribution,* 13: 1–12.

Lomolino, M. V. 2001. Elevation gradients of species richness, historical and prospective views. *Global ecology and biogeography*, 10:3-13.

Lomolino, M.V., Sax, D.F. and Brown, J.H. 2004. *Foundations of biogeography: classic papers with commentaries*, Chicago, University of Chicago Press.

Luoto, M., Toivonen, T. and Heikkinen, R.K. 2002. Prediction of total and rare plant species richness in agricultural landscapes from satellite images and topographic data. *Landscape Ecol.,* 17: 195-217.

Magurran, A.E. 1988. *Ecological diversity and its measurements*, Princeton University Press, New Jersey.
Marquardt, D. W. 1970. Generalized inverses, ridge regression, biased linear estimation, and nonlinear estimation. *Technometrics,* 12: 591–256.
Marsden, S. J. and Pilgrim, J. D. 2003. Diversity and abundance of fruiting trees in primary forest, selectively logged forest, and gardens on New Britain, Papua New Guinea. *Tropical biodiversity,* 8(1): 15-29.
Martin, M.E., Newman, S.D., Aber, J.D. and Congalton, R.G. 1998. Determining forest species composition using high spectral resolution remote sensing data. *Remote Sensing of Environment*, 65: 249–54.
Mason, R. L., Gunst, R. F. and Hess, J. L. 1989. *Statistical Design and Analysis of experiments,* John Wiley.
Mcgarigal, K., Cushman, S. and Stafford, S., 2000, *Multivariate Statistics for Wildlife and Ecology Research,* New York, Springer.
Mehner, H., Cutler, M., Fairbairn, D., and Thompson, G. 2004. Remote sensing of upland vegetation: The potential of high spatial resolution satellite sensors. *Global Ecology and Biogeography*, 13, 359−369.
Menard, S. 1995. *Applied logistic regression analysis,* Sage University Paper series on Quantitative Applications in the Social Sciences, Sage, Beverly Hills, CA.
Meyer, P., Staenz, K. and Itten, K.I. 1996. Semi-automated procedures for tree species identification in high spatial resolution data from digitized colour infrared-aerial photography. *Photogrammetric Engineering and Remote Sensing,* 51:5-16.
Mouillot, D., Leprêtre, A. 1999. A comparison of species diversity estimators. *Researches on Population Ecology,* 41: 203-215.
Mutanga, O and Kumar, L. 2007. Estimating and mapping grass phosphorus concentration in an African savanna using hyperspectral image data. *International Journal of Remote Sensing*, 28(21): 4897–4911.
Mutanga, O. and Rugege, D. 2006. Integrating remote sensing and spatial statistics to model herbaceous biomass distribution in a tropical savanna. *International Journal of Remote Sensing,* 27(16): 3499–3514.
Nagendra, H. 2001. Using remote sensing to assess biodiversity. *International Journal of Remote Sensing*, 22:2377−2400.
Nagendra, H. 2002. Using remote sensing to assess biodiversity. *International Journal of Remote Sensing*, *22*(12):2377–2400.
Nagendra, H. and Gadgil, M. 1999a. Satellite imagery as a tool for monitoring species diversity: an assessment. *Journal of Applied Ecology*, 36:388-397.
Nagendra, H. and Gadgil, M. 1999b. Biodiversity assessment at multiple scales: Linking remotely sensed data with field information. *Ecology,* 96:9154-9158.
Nahal, I. 1981. The Mediterranean climate from a biological viewpoint. In di Castri, F., Goodall, D. W. and Specht, R. L. (Eds.), *Ecosystems of the world 11. Mediterranean type shrublands*, 63–86 pp.
O'Brien, E M., Field, R. and Whittaker, R. J. 2000. Climatic gradients in woody plant (tree and shrub) diversity: water energy dynamics, residual variation and topography. *Oikos*, 89 (3): 588-600.

O'brien, R. M. 2007. A Caution Regarding Rules of Thumb for Variance Inflation Factors. *Quality and Quantity*, 41:673–690.
O'dae, N., Whittaker, R. J. and Ugland, K. I. 2006. Using spatial heterogeneity to extrapolate species richness: a new method tested on Ecuadorian cloud forest birds. *Journal of Applied Ecology*, 43:189-198.
Oindo, B.O. and Skidmore, A.K. 2002. Interannual variability of NDVI and species richness in Kenya. *Int. J. Remote Sens.,* 23: 285-298.
Ǿkland, R.H. 1990. *Vegetation ecology: theory, methods and applications with reference to Fennoscandia. Sommerfeltia Supplement,* 1: 1-123.
Onaindia, M., Dominguez, I., Albizu, I., Garbisu, C., Amezaga, I. 2004. Vegetation diversity and vertical structure as indicators of forest disturbance. *Forest Ecology and Management,* 195:341-354.
Palmer, M.W., Earls, P., Hoagland, B.W., White, P.S. and Wohlgemuth, T. 2002. Quantitative tools for perfecting species lists. *Environmetrics,* 13: 121-137.
Parco Nationale della Majella. 1999. Realizzazione degli studi preliminarie e dell'elaborato technico del piano del parco e del regolamento. Volume 2.
Parikh, J. A., DaPonte, J. S., Damodaran, D., Karageorgiou, A. and Podaras P. 1991. Comparison of backpropagation neural networks and statistical techniques for analysis of geographical features in Landsat imagery. *SPIE-Application of Artificial Neural Networks II*, 1469: 526-538.
Pielou, E. C., 1975. Ecological diversity. John Wiley and Sons, INC, 165p.
Pierce, K. B., Lookingbill, T and Urban, D. A simple method for estimating potential relative radiation (PRR) for landscape-scale vegetation analysis. *Landscape Ecology*, 20:137-147.
Price, J.C. 1994. How unique are spectral signatures? *Remote Sensing of Environment*, 49: 181-186.
Purvis, A., Hector, A., 2000. Getting the measure of biodiversity. *Nature*, 405: 212–219.
Ramsey, E., Rangoonwala, A., Nelson, G., Ehrlich, R. and Martella, K. 2005. Generation and validation of characteristics spectra from EO1 Hyperion image data for detecting the occurrence of the invasive species, Chinese tallow. *International Journal of Remote Sensing,* 26:1611–36.
Richerson, P. J. and Lum, K. L. 1980. Patterns of plant species diversity in California: relation to weather and topography. *American Naturalist*, 116: 504-536.
Rindfuss, R.R., Walsh, S.J., Turner, B.L., Fox. J. and Mishra, V. 2004. Developing a science of land change: challenges and methodological issues. *Proceedings of the National Academy of Sciences of the United States of America,* 101: 13976–81.
Rocchini, D. 2007. Effects of spatial and spectral resolution in estimating ecosystem α-diversity by satellite imagery. *Remote Sensing of Environment,* 111: 423–434.
Rocchini, D., Chiarucci, A. and Loiselle, S.A. 2004. Testing the spectral variation hypothesis by using satellite multispectral images. *Acta Oecol.,* 26: 117-120.
Rocchini, D., Ricotta, C. and Chiarucci, A. 2007. Using satellite imagery to assess plant species richness: The role of multispectral systems. *Applied Vegetation Science*, 10:325-332.
Rossiter, D.G. 2004. Technical Note: Statistical methods for accuracy assessment of classified thematic maps. *Technical Report ITC*, Enschede, NL. April 2004, 46 p.

Runkle, J.R. 1982. Patterns of Disturbance in Some Old-Growth Mesic Forests of Eastern North America. *Ecology*, 63: 1533-1546.

Saatchi, S., Buermann, W., Mori, S., ter Steege, H. and Smith, T. 2008. Modeling distribution of Amazonian tree species and diversity using remote sensing measurements. *Remote Sensing of the Environment*, 112 (5): 2000-2017.

Sager, P . E . and Hasler, A. D . 1969 . Species diversity in lacustrine phytoplankton. I. The components of the index of diversity from Shannon's formula. *The American Naturalist*, 103: 51-59.

Salvador, R. and Pons, X. 1998. On the applicability of TM images to Mediterranean forest inventories. *Forest Ecology and Management,* 104: 193–208.

Sanjit, L. and Bhatt, D. 2005. How relevant are the concepts of species diversity and species richness? *Journal of Biosciences*, 30 (5): 557-560.

Schmidt, K. S., Skidmore, A. K., Kloosterman, E. H. van Oosten,H., Kumar, L. and Janssen, J. A. M. 2004. Mapping Coastal Vegetation Using an Expert System and Hyperspectral Imagery. *Photogrammetric Engineering and Remote Sensing*, 70 (6): 703–715.

Schmidtlein, S. and Sassin, J. 2004. Mapping of continuous floristic gradients in grasslands using hyperspectral imagery. *Remote Sensing of Environment,* 92: 126–38.

Shannon, C.E. 1948. A mathematical theory of communication. *Bell Syst. Tech. J.*, 27: 379–423.

Skidmore, A., Turner, B. J., Brinkhof, W. and Knowles, E. 1997. Performance of Neural Network:Mapping Forest Using GIS and Remotely Sensed Data. *Photogrammetric Engineering and Remote Sensing*, 63(5): 501-514.

Skidmore, A.K. 1989. An expert system classifies Eucalypt forest types using Thematic Mapper data and a digital terrain model. *Photogrammetric Engineering and Remote Sensing,* 55(10): 1449-1464.

Skidmore, A.K. 1999. Accuracy assessment of spatial information. In A. Stein, F. van der Meer and B. Gorte (Eds), *Spatial Statistics for Remote Sensing*, (Dordrecht: Kluwer Academic), 197–209 pp.

Skidmore, A.K., Turner, B.J., Brinkhof, W. and Knowles, E. 1997. Performance of a neural network: mapping forests using GIS and remotely sensed data. *Photogrammetric Engineering and Remote Sensing*, 63: 501–514.

Sobhan M. I. 2007. Species discrimination from a hyperspectral perspective. *PhD Thesis,* Faculty of Geo-Information Science and Earth Observation (ITC), Enschede, University of Twente, the Netherlands.

Stanisci, A., Pelino, G. and Blasi, C. 2005. Vascular plant diversity and climate change in the alpine belt of the central Apennines (Italy). *Biodiversity and Conservation*, 14: 1301–1318.

Stirling, G. and Wilsey, B. 2001. Empirical Relationships between Species Richness, Evenness, and Proportional Diversity. *The American Naturalist,* 138(3):286-299.

Tilman, D. 1996. Biodiversity: Population Versus Ecosystem Stability. *Ecology*, 77(2):350-363.

Tivy, J. 1993. *Biogeography - A study of plants in the ecosphere*, Longman, Harlow.

Tolera, M., Asfaw, Z., Lemenih, M., Karltun, E. 2008. Woody species diversity in a changing landscape in the south-central highlands of Ethiopia. *Agriculture Ecosystems and Environment*, 128: 52-58.

Trisurat, Y., Eiumnoh, A., Murai, S., Hussain, M.Z. and Shrestha R.P. 2000. Improvement of tropical vegetation mapping using a remote sensing technique: a case of Khao Yai National Park, Thailand. *International Journal of Remote Sensing,* 21:2031–42.

Turner, W., Spector, S., Gardiner, N., Fladeland, M., Sterling, E. and Steininger, M. 2003. Remote sensing for biodiversity science and conservation. *Trends in Ecology and Evolution,* 18:306–14.

Ubaldi, D., Zanotti, A.L., Puppi, G. 1995. Les paysages forestie` res de l'Emilie Romagne et leur signification bioclimatique. *Colloques Phytosociologiques,* 21: 269–286.

van Gils, H., Batsukh, O., Rossiter, D., Munthali, W. and Liberatoscioli, E. 2008. Forecasting the pattern and pace of Fagus forest expansion in Majella National Park, Italy. *Applied Vegetation Science,* 11:539-546.

van Gils, H., Odoi, J. O. and Andrisano, T. 2010. From monospecific to mixed forest after fire? An early forecast for the montane belt of Majella, Italy. *Forest Ecology and Management*, 259:433–439.

Verbyla, D.L. 1995. *Satellite remote sensing of natural resources*, 1st edn, Lewis Publishers, New York.

Vogiatzakis, I.N., Mannion, A.M. and Griffiths, G.H. 2006. Mediterranean ecosystems: problems and tools for conservation. *Progress in Physical Geography,* 30: 175–200.

Wallace, A. R. 1878. *Tropical nature and other essays*, Macmillan, New York.

Wang, L., Sousa, W., Gong, P. 2004b. Integration of object-based and pixel-based classification for mangrove mapping with IKONOS imagery. *International Journal of Remote Sensing*, 25(24): 5655–5668.

Wang, L., Sousab, W.P., Gong, P. and Biging, G.S. 2004. Comparison of IKONOS and QuickBird images for mapping mangrove species on the Caribbean coast of Panama. *Remote Sensing of the Environment,* 91:432–40.

Wang, Q., Ni, J. and Tenhunen, J. 2005. Application of a geographically-weighted regression analysis to estimate net primary production of Chinese forest ecosystems. *Global Ecol. Biogeogr.,* 14: 379-393.

Waser, L.T., Stofer, S., Schwarz, M., Küchler, M., Ivits, E. and Scheidegger, C.H. 2004. Prediction of biodiversity: regression of lichen species richness on remote sensing data. *Community Ecology,* 5: 121–34.

Whittaker, R. H. 1972. Evolution and measurement of species diversity. *Taxon*, 21 (2): 213-251.

Whittaker, R. H. 1975. *Communities and Ecosystems,* 2nd Edition, MacMillan Publishing Co., New York, 385p.

Whittaker, R.H. 1965. Dominance and Diversity in Land Plant Communities. *Science,* 147:250-260.

Whittaker, R.J. Araújo, M.B., Jepson, P., Ladle, R.J., Watson, J.E.M. and Willis, K.J. 2005. Conservation biogeography: Assessment and prospect. *Diversity and Distribution,* 11: 3–23.

Willis, K.J. and Whittaker, R.J. 2002. Species diversity-scale matters. *Science,* 295:1245–48.
Xu, B., Gong, P and Pu, R. 2003. Crown closure estimation of oak savannah in a dry season with TM imagery: comparison of various indices through correlation analysis. *International Journal of Remote Sensing,* 24 (9): 1811-1822.
Yamamoto, Y., Oberthur, T. and Lefroy, R. 2009. Spatial identification by satellite imagery of the crop–fallow rotation cycle in northern Laos. *Environ Dev Sustain*, 11:639–654.
Yang, X., Skidmore, A. K., Melick, D., Zhou, Z. and Xu, J. 2007. Towards an efficacious method of using Landsat TM imagery to map forest in complex mountain terrain in Northwest Yunnan, China. *Tropical Ecology,* 48(2): 227-239.
Yoccoz, N.G., Nichols, J.D. and Boulinier, T. 2001. Monitoring of biological diversity in space and time. *Trends Ecol. Evol.,* 16: 446-463.
Zhang, J.T., Pennington, D.D. and Liu, X.H. 2007. GBD-Explorer: extending open source java GIS for exploring ecoregion-based biodiversity data. *Ecological Informatics,* 2: 94–102.

Appendices

Appendix 1: Multicollinearity assessment

Layer	Collinearity Statistics	
	Tolerance	VIF
DEM	.340	2.941
SLOPE	.531	1.883
ASPECT	.485	2.061
SOLAR RADIATION	.313	3.194
TM BAND 1	.160	6.269
TM BAND 2	.131	7.660
TM BAND 4	.281	3.558
TM BAND 6	.200	5.010

Appendix 2: Multicollinearity assessment for ALOS

	Collinearity Statistics	
Layer	Tolerance	VIF
DEM	.387	2.583
ASPECT	.651	1.536
SLOPE	.592	1.689
SOLAR RADIATION	.495	2.022
ALOS BAND 1	.121	8.266
ALOS BAND 2	.140	7.126
ALOS BAND 4	.340	2.943

Appendix 3: Mapping accuracy comparison of Shannon diversity index (H) obtained from the confusion matrices resulted in neural network by using band 1, 2, 4 and 6 of TM (TM-Multi) and bands 1, 2 and 4 of ALOS (ALOS Multi) which do not have multicollinearity problem, with respective accuracy resulted by using all bands of TM (TM_ALL) and ALOS (ALOS_ALL), ordered by Overall Accuracy (OA%) of TM Multi.

	OA%				Kappa			
	TM Multi	TM All	ALOS Multi	ALOS All	TM Multi	TM All	ALOS Multi	ALOS All
1. IMAGE+ASPECT+DEM+SLOPE+SOLAR RADIATION	87	91	80	81	0.84	0.89	0.75	0.77
2. IMAGE+ASPECT+DEM+SLOPE	86	87	77	80	0.82	0.84	0.71	0.75
3. IMAGE+DEM+SLOPE+SOLAR RADIATION	86	86	76	79	0.82	0.82	0.70	0.73
4. IMAGE+SOLAR ADIATION+SLOPE	83	83	73	73	0.79	0.79	0.66	0.66
5. IMAGE+DEM+ASPECT+SOLAR RADIATION	81	83	74	76	0.77	0.79	0.68	0.70
6. IMAGE+SLOPE+ASPECT+SOLAR RADIATION	81	81	80	81	0.77	0.77	0.75	0.75
7. IMAGE+SLOPE	80	86	64	64	0.75	0.82	0.55	0.55
8. IMAGE+SOLAR ADIATION+DEM	80	84	71	74	0.75	0.80	0.64	0.68
9. IMAGE+DEM+SLOPE	80	80	74	77	0.75	0.75	0.68	0.71
10. IMAGE+ASPECT+SLOPE	79	80	76	74	0.73	0.75	0.70	0.68
11. IMAGE+ASPECT+DEM	77	81	70	74	0.71	0.77	0.63	0.68
12. IMAGE+SOLAR ADIATION+ASPECT	74	77	73	70	0.68	0.71	0.66	0.63
13. IMAGE+DEM	71	66	64	67	0.64	0.57	0.55	0.59
14. IMAGE+SOLAR RADIATION	70	70	69	69	0.63	0.63	0.61	0.61
15. IMAGE+ASPECT	66	67	66	69	0.57	0.59	0.57	0.61
16. IMAGE	56	60	49	53	0.45	0.50	0.36	0.41

Appendix 4: Mapping accuracy comparison of Shannon diversity (H) index obtained by using overlapping 4 bands TM (TM-4) against 6 bands of TM (TM-6) and ALOS imageries, from the confusion matrix resulted in neural network, and ordered by Overall Accuracy (OA%) of TM-4.

	OA%			Kappa		
	TM-4	TM-6	ALOS	TM-4	TM-6	ALOS
1. IMAGE+ASPECT+DEM+SLOPE+SOLAR RADIATION	84	91	81	0.80	0.89	0.77
2. IMAGE+ASPECT+DEM+SLOPE	81	87	80	0.77	0.84	0.75
3. IMAGE+SOLAR ADIATION+SLOPE	80	83	73	0.75	0.79	0.66
4. IMAGE+DEM+SLOPE	80	80	77	0.75	0.75	0.71
5. IMAGE+DEM+ASPECT+SOLAR RADIATION	80	83	76	0.75	0.79	0.70
6. IMAGE+DEM+SLOPE+SOLAR RADIATION	80	86	79	0.75	0.82	0.73
7. IMAGE+SLOPE+ASPECT+SOLAR RADIATION	80	81	80	0.75	0.77	0.75
8. IMAGE+ASPECT+DEM	79	81	74	0.73	0.77	0.68
9. IMAGE+SOLAR ADIATION+DEM	77	84	74	0.71	0.80	0.68
10. IMAGE+ASPECT+SLOPE	77	80	74	0.71	0.75	0.68
11. IMAGE+SLOPE	74	86	64	0.68	0.82	0.55
12. IMAGE+SOLAR ADIATION+ASPECT	73	77	70	0.66	0.71	0.63
13. IMAGE+SOLAR RADIATION	71	70	69	0.64	0.63	0.61
14. IMAGE+DEM	71	66	67	0.64	0.57	0.59
15. IMAGE+ASPECT	67	67	69	0.59	0.59	0.61
16. IMAGE	53	60	53	0.41	0.50	0.41

Appendix 5: Mapping accuracy comparison of Shannon evenness index (E) obtained from the confusion matrices resulted in neural network by using band 1, 2, 4 and 6 of TM (TM-Multi) and bands 1, 2 and 4 of ALOS (ALOS Mulit) which do not have multicollinearity problem, with respective accuracy resulted by using all bands of TM (TM_ALL) and ALOS (ALOS_ALL), ordered by overall accuracy (OA%) of TM Multi

	Overall accuracy %				Kappa Coefficients			
	TM Multi	TM All	ALOS Multi	ALOS All	TM Multi	TM All	ALOS Multi	ALOS All
1. IMAGE+ASPECT+DEM+SLOPE+SOLAR RADIATION	81	83	80	80	0.77	0.79	0.75	0.75
2. IMAGE+ASPECT+DEM+SLOPE	79	81	73	74	0.73	0.77	0.66	0.68
3. IMAGE+DEM+SLOPE+SOLAR RADIATION	79	79	71	71	0.73	0.73	0.64	0.64
4. IMAGE+SLOPE+ASPECT+SOLAR RADIATION	77	81	76	76	0.71	0.77	0.70	0.70
5. IMAGE+ASPECT+DEM	76	79	66	67	0.70	0.73	0.57	0.59
6. IMAGE+SOLAR ADIATION+DEM	76	79	67	76	0.70	0.73	0.59	0.70
7. IMAGE+SOLAR RDIATION+SLOPE	76	79	66	69	0.70	0.73	0.57	0.61
8. IMAGE+DEM+ASPECT+SOLAR RADIATION	74	77	73	77	0.68	0.71	0.66	0.71
9. IMAGE+DEM+SLOPE	73	79	69	69	0.66	0.73	0.61	0.61
10. IMAGE+ASPECT+SLOPE	71	73	66	71	0.64	0.66	0.57	0.64
11. IMAGE+SLOPE	70	73	61	63	0.63	0.66	0.52	0.54
12. IMAGE+SOLAR RADIATION	70	69	61	67	0.63	0.61	0.52	0.59
13. IMAGE+SOLAR ADIATION+ASPECT	70	77	64	63	0.63	0.71	0.55	0.54
14. IMAGE+DEM	69	70	56	54	0.61	0.63	0.45	0.43
15. IMAGE+ASPECT	59	71	57	61	0.48	0.64	0.46	0.52
16. IMAGE	53	59	40	46	0.41	0.48	0.25	0.32

Appendix 6: Mapping accuracy comparison of Shannon evenness index (E) obtained by using overlapping 4 bands TM (TM-4) against 6 bands of TM (TM-6) and ALOS imageries, from the confusion matrices resulted in neural network, and ordered by overall accuracy (OA%) of TM-4.

	Overall accuracy %			Kappa		
	TM_4	TM_6	ALOS	TM_4	TM_6	ALOS
1. IMAGE+ASPECT+DEM+SLOPE+SOLAR RADIATION	83	83	80	0.79	0.79	0.75
2. IMAGE+ASPECT+DEM+SLOPE	80	81	74	0.75	0.77	0.68
3. IMAGE+DEM+SLOPE+SOLAR RADIATION	79	79	71	0.73	0.73	0.64
4. IMAGE+SOLAR RDIATION+SLOPE	77	79	69	0.71	0.73	0.61
5. IMAGE+SLOPE+ASPECT+SOLAR RADIATION	77	81	76	0.71	0.77	0.70
6. IMAGE+SOLAR ADIATION+ASPECT	76	77	63	0.70	0.71	0.54
7. IMAGE+SOLAR ADIATION+DEM	76	79	76	0.70	0.73	0.70
8. IMAGE+DEM+SLOPE	76	79	69	0.70	0.73	0.61
9. IMAGE+DEM+ASPECT+SOLAR RADIATION	76	77	77	0.70	0.71	0.71
10. IMAGE+SLOPE	73	73	63	0.66	0.66	0.54
11. IMAGE+ASPECT+SLOPE	73	73	71	0.66	0.66	0.64
12. IMAGE+ASPECT+DEM	71	79	67	0.64	0.73	0.59
13. IMAGE+DEM	69	70	54	0.61	0.63	0.43
14. IMAGE+ SOLAR RADIATION	69	69	67	0.61	0.61	0.59
15. IMAGE+ASPECT	66	71	61	0.57	0.64	0.52
16. IMAGE	57	59	46	0.46	0.48	0.32

Author's Biography

Mohammad Redowan was born on 27th Dec 1977 and brought up at Habigonj district in Bangladesh. He obtained Bachelor of Science degree with honours in 2004 and Master of Science degree in 2005 in Forestry from the Institute of Forestry and Environmental Sciences in Chittagong University (IFESCU), Bangladesh. He joined on March 2005 as a lecturer in the Department of Forestry and Environmental Sciences (DFES) in the Shahjalal University of Science and Technology (SUST), the largest public university of its kind in Bangladesh. Currently he is working as an Assistant Professor. In 2008, Mr. Redowan received the European Union Erasmus Mundus scholarship for the MSc in 'Geo-information Science and Earth Observation for Environmental Modelling and Management (GEM)' a course jointly organized by a consortium of four partner universities of four European countries. He was granted study leave from the DFES to pursue the program, in partial fulfilment of which this thesis was completed. His teaching and research points of interest include application of remote sensing and GIS in forestry, research methods, forest and environmental modelling.

Contact:

Professional address:

Mohammad Redowan
Department of Forestry and Environmental Science
Shahjalal University of Science and Technology (SUST)
Sylhet-3114, Bangladesh
Tel: PABX.0821-713491, 713850/ extn.-273
Fax: 88-0821-715257
Email: redowanforestry@yahoo.com
: redowan-for@sust.edu
Cell: +880-1818465634

Home address:

Mohammad Redowan
C/O Mohammad Sirajul Islam
Holding No 72/73
Shayestanagar Traffic Point (east side)
Habigonj-3300
Bangladesh.